Evaluation and Mitigation of Power System Oscillations

Arising from High Solar Penetration

by

Anushree Sanjeev Pethe

A Thesis Presented in Partial Fulfillment
of the Requirements for the Degree
Master of Science

Approved November 2014 by the
Graduate Supervisory Committee:

Gerald Heydt, Co-Chair
Vijay Vittal, Co-Chair
Raja Ayyanar

ARIZONA STATE UNIVERSITY

May 2015

ABSTRACT

An important operating aspect of all transmission systems is power system stability and satisfactory dynamic performance. The integration of renewable resources in general, and photovoltaic resources in particular into the grid has created new engineering issues. A particularly problematic operating scenario occurs when conventional generation is operated at a low level but photovoltaic solar generation is at a high level. Significant solar photovoltaic penetration as a renewable resource is becoming a reality in some electric power systems. In this thesis, special attention is given to photovoltaic generation in an actual electric power system: increased solar penetration has resulted in significant strides towards meeting renewable portfolio standards. The impact of solar generation integration on power system dynamics is studied and evaluated.

This thesis presents the impact of high solar penetration resulting in potentially problematic low system damping operating conditions. This is the case because the power system damping provided by conventional generation may be insufficient due to reduced system inertia and change in power flow patterns affecting synchronizing and damping capability in the AC system. This typically occurs because conventional generators are rescheduled or shut down to allow for the increased solar production. This problematic case may occur at any time of the year but during the springtime months of March-May, when the system load is low and the ambient temperature is relatively low, there is the potential that over voltages may occur in the high voltage transmission system. Also, reduced damping in system response to disturbances may occur. An actual case study is

considered in which real operating system data are used. Solutions to low damping cases are discussed and a solution based on the retuning of a conventional power system stabilizer is given in the thesis.

ACKNOWLEDGEMENTS

Firstly, I would like to thank Salt River Project (SRP) for their financial assistance. SRP is one of Arizona's largest power utilities and has assisted me in obtaining my graduate degree.

Secondly, I would like to thank my advisors Dr. Vijay Vittal and Dr. Gerald Heydt. With their support and constant motivation I was able to make all of this possible. Their encouragement, guidance and supervision helped me balance and complete my work. I also thank Dr. Raja Ayyanar for his time in being a part of my graduate supervisory committee.

Lastly, I would like to thank my family and friends for being there for me through thick or thin. My parents' love and motivation and my friends' support helped me get through graduate school. I am very grateful to them.

TABLE OF CONTENTS

CHAPTER Page

LIST OF FIGURES

Figure Page

Figure Page

Figure Page

LIST OF TABLES

Table Page

Table Page

NOMENCLATURE

A, B, C, D	Row matrices of all dynamic device matrices A_d , B_d , C_d , D_d
A_d , B_d , C_d , D_d	Matrices of each dynamic device in the system
A', B', C', D'	System matrices after elimination of rotor angle and speed terms
A_{sys} , B_{sys} , C_{sys} , D_{sys}	System matrices
ALEC	American Legislative Exchange Council
α	Corresponding value of lead/lag time constant T_1 and T_3
CT	Combustion turbine
D	Damping
D_0	Step change in regulator output
$\Delta E'_q$	q-axis transient voltage
ΔE_{fd}	Excitation system voltage
ΔE_{pss}	Power system stabilizer voltage deviation
ΔE_{ref}	Input voltage to the excitation system
$EXC(s)$	Exciter function
f	Frequency
F_d	Response input vector
$\psi_{fd}, \psi_{kd1}, \psi_{kq1}, \psi_{kq2}$	Rotor circuit flux linkages as generator states
$GEP(s)$	Excitation system transfer function
GT	Gas turbine

$G_s(s)$	Generator-exciter transfer function in Section 2.3 equation (2.8)
I-V	Current versus Voltage
i_d	Currents injected into the network at the device terminals
K_s	Stabilizer gain
$K_1 – K_6$	DeMello-Concordia constants
M	Inertia coefficient
PSS	Power System Stabilizer
$PSS_\omega(s)$	Power system stabilizer function
PV	Photovoltaic
P_{ref}	Governor reference input power
P-V	Power versus voltage
RPS	Renewable Portfolio Standards
s	Laplace transform variable
SRP	Salt River Project
SSAT	Small Signal Analysis Tool
SVC	Static Var Compensators
TSAT	Transient Security Assessment Tool
T_e	Electrical torque
$T_1 – T_4$	Lead/Lag time constants
T_5	Washout time constant
τ	Corresponding value of lead/lag time constant T_2 and T_4

t_0	Specific time in a time-invariant dynamic system
T'_{d0}	Open circuit d-axis time constant
ΔT_m	Mechanical torque
u	Input vector
v_d	Voltage vector of voltages at the device terminal bus and any remote sensing buses
V_{ref}	Exciter reference input voltage
WECC	Western Electricity Coordinating Council
x	State vector
$\dot{x}$	Derivative of x
x_d	State vector of each dynamic device
$\dot{x}_d$	Derivative of x_d
X	Variable used in MATLAB curve-fitting function
x_0	Initial state of a time-invariant dynamic system
x_{TF}, x_{TB}, x_{TA}	Winding reactance as exciter states
x_d	Representation of generator-exciter states
Y	Output vector
$Y(X)$	Curve-fitting function to tune PSS
Y_n	Reduced network admittance matrix
Θ	Phase lead to compensate the phase lag in PSS tuning
Ω	Frequency in radians per second

$\Delta\overline{\omega}_g$	Machine's speed deviation
ω_b	Rotor speed deviation
Δ	Generator rotor angle
$\Delta\delta$	Rotor angle deviation of synchronous generator

CHAPTER 1 PROJECT DESCRIPTION AND INTRODUCTION

1.1 The scope of this thesis

This thesis investigates the impact of solar PV generation on power system dynamics. Since renewable sources of energy are gaining importance over the years (solar generation being one of the major renewable sources), solar PV generation is integrated into the grid and an equal amount of conventional generation has to be rescheduled or shut down to accommodate PV generation. As a result, the system experiences loss of inertia which can result in over-voltages and slightly reduced damping of system oscillation. These are not beneficial for the system. This thesis studies the impact of PV generation on system oscillations and implements measures to improve the system damping of oscillations. Some of this work was summarized and reported in the North American Power Symposium [23].

1.2 Motivation and description

This study is done for a large power company using actual data. The study assumes that significant solar penetration has occurred in their service territory. Increased solar penetration has resulted in significant strides towards meeting renewable portfolio standards (RPS). Significant penetration of solar generation during periods of low service territory generation during the months of March – May when the load in the service territory is low has a tendency to cause overvoltages in the high voltage system and also result in slightly reduced damping in system response to disturbances. One aspect which contributes to this reduced damping is that conventional generators have to be rescheduled or shut down to allow for the increased solar penetration. This results in significantly different operating

conditions for which power system stabilizers (PSSs) (which exist on conventional generators) may not have been adequately tuned.

In this research, the following were studied:

- Examine range of operating conditions with increased penetration of solar generation and low valley generation to ascertain damping achieved by existing settings on PSS
- Conduct a sensitivity analysis and evaluate how damping changes with change in solar penetration
- Tune PSS
- Test the new settings of the PSS and examine performance for cases which showed low damping with existing PSS settings

The following are the main research objectives:

- Examining operating conditions with increased penetration of solar generation that result in reduced damping of oscillations.
- Conducting small signal stability analysis on these cases and evaluating the damping performance of existing PSS settings.
- Conducting a sensitivity analysis of damping performance with change in solar penetration.
- Retuning existing PSS settings.
- Testing the performance of the retuned PSS settings.

1.3 Background literature

- Solar PV generation

Solar and other renewable resources have gained significant importance as energy sources owing to the increase in population over the years and the rise in demand for energy. The exhaustive nature of non-renewable resources such as fossil fuels has made it imperative to find alternate ever-lasting sources of energy generation. Using solar PV to generate electricity is one of the effective means of solving problems related to exhaustion of energy resources, and environmental pollution. The technical problems with PV power generation are analyzed and suggestions for improvement are provided in [13]. Further, the PV power generation system is analyzed to improve design and efficiency. Methods to increase solar PV generation have been implemented. Maximum installation capacity of solar PV systems by applying active and reactive power controls increases penetration in power distribution systems [14]. Based on PV active power injection and the loading, the voltage magnitude and voltage variation ratio at each bus are obtained by applying power flow analysis for determining the maximum PV installation capacity.

For effective energy extraction from a solar PV system, the I-V and P-V characteristics of solar PV cells and modules are studied [15]. The study considers the relationship between semiconductor properties of solar PV system and the external electric circuit requirements.

Limitations encountered in implementing solar PV generation cannot be ignored. The status and needs related to optimizing the integration of electrical energy storage and grid-connected PV systems are assessed [16]. At high levels of PV penetration on the

electric grid, reliable and economical distributed energy storage eliminates the need for back-up utility generation capacity to offset the intermittent nature of PV generation. The status of various storage technologies in the context of PV system integration, addressing applications, benefits, costs and technology limitations is summarized. Further research and development needs, with emphasis on new models, systems analysis tools, and even business models for high penetration of PV storage systems is also discussed.

The electric power industry will undergo a radical change as the RPS of several states will be implemented during the next decade. Now that over half the states in the U.S. have adopted aggressive RPS, the issues of reliable penetration of dispersed renewables into the grid have become a major topic of discussion [17]. The major challenge facing the U.S. electric power industry is fulfilling its obligations to be simultaneously reliable, economical and environmentally friendly as it grows under the RPS requirements, deregulation and industry restructuring.

As per the model bill, the Electricity Freedom Act, drafted by ALEC, the states in the U.S.A. would be required to derive a specific percentage of their electricity needs from renewable energy sources [18]. The RPS of some of the states in WECC are shown in Table 1.1.

Table 1.1 RPS of some states in WECC

State	Amount (%)	Year
Arizona	15	2025
California	25, 33	2016, 2020
Colorado	30	2020
Montana	15	2015
Nevada	25	2025
New Mexico	20	2020

- Impacts of solar PV generation on power system stability and damping performance

Solar PV power generating systems are fundamentally different from conventional synchronous generators. Photovoltaics produce direct current and the interface with the grid is via an electronic inverter. Photovoltaic resources do not have inertia and their dynamic behavior is dominated by the characteristics of the power electronic inverters. Increased solar PV generation can either have beneficial or detrimental effects on small signal stability depending on the location and penetration level of solar PV generation and the dispatch of existing conventional synchronous generators. Impact of solar PV generation on small signal stability is studied in [19].

Solar PV generation can cause potential voltage and stability issues. Solar PV generation interconnections may cause oscillation problems following faults, high voltage problems in sub-transmission and distribution systems under normal conditions, and transient over-voltage in the grid following faults [20]. These problems may further cause reliability concerns such as overload of sub-transmission and distribution lines, over-voltage

generation tripping, and transient instability. At low levels of penetration, none of these issues are present, but at high levels of penetration, there is a reasonable motivation to study and assess the problematic issues indicated. When oscillation problems arise in the system due to large solar PV integration, critical synchronous generators need to be kept on-line or other measures such as SVC or power system stabilizer tuning, need to be taken to maintain sufficient damping of these low frequency oscillations [19].

Voltage stability studies are carried out using PV curves and small-perturbation stability studies are performed (based on eigenvalue analyses of linearized system models), and time-domain studies are carried out to examine the overall performance of the system in case of contingencies. This is the general approach taken in [21].

1.4 Organization of this thesis

Chapter 1 begins with the scope of the topic of research. It further introduces the impacts of high solar PV generation on power system stability and damping of low frequency oscillations. Chapter 2 explains the Larsen and Swann method of PSS tuning. The advantages of these methods are also discussed along with the reason for not implementing the Larsen and Swann method of power system stabilizer tuning. Chapter 3 discusses the 2010 spring light load case in details. The base case scenario and the scenarios with changing PV penetration are analyzed. Varying levels of PV generation are considered. The impacts on frequency and damping of oscillations are observed. Results obtained by eigenvalue analysis are verified using time domain simulations. Corrective measures to improve the damping are implemented. The improvement in damping is observed graphically. Chapter 4 follows-up on the approach and analysis taken in Chapter 3 except

that the 2018 summer peak load data is considered and analyzed. Chapter 5 summarizes the conclusions and is followed by references.

The tests to shut down conventional generation (Test 1 – Test 3), retune PSS (Test 4) and carry out time domain analysis (Test 5) are given in Appendix A. Appendix B gives the MATLAB code for the example of PSS design (shown in Chapter 2) using the Larsen and Swann method of PSS tuning.

CHAPTER 2 THE LARSEN AND SWANN METHOD FOR PSS TUNING

2.1 Power system damping and the role of a power system stabilizer

An electrical power system is a network of electrical components used to generate, transmit, supply and use electric power. For AC power systems, power system stability is an important operating consideration. The performance of a power transmission system depends on its various components like generation and excitation units, loads, capacitors and reactors, power electronic devices, and protective devices [2]. While the system reliability is high, excitation systems with high gain and low time constants may initiate low frequency oscillations that may persist for long periods of time and cause limitations in transmitting power. Power system stabilizers are used to provide damping for these undesirable oscillations.

The basic function of a PSS is to provide damping to system oscillations via modulation of generator excitation. The oscillations of concern typically occur in the frequency range of approximately 0.2 to 2.5 Hz, and insufficient damping of these oscillations may limit power transfer capability [2]. A PSS takes local inputs (speed, frequency, voltage, power) and provides an auxiliary signal to damp oscillations. For any input signal the transfer function of the stabilizer should compensate for the gain and phase characteristics of the excitation system, the generator and the power system itself. The input signal determines the transfer function from the control input to the excitation system to the component of electrical torque which can be modulated via excitation control. The exciter transfer function is influenced by voltage regulator gain, generator power level and the AC system itself.

2.2 The Larsen and Swann method of PSS tuning

PSS tuning is an important concept. Tuning of PSS consists of obtaining correct parameters to achieve satisfactory performance of the power system. Tuning of PSS helps provide an auxiliary signal to damp oscillations. This is done by adjusting the lead/lag parameters of the PSS depending on the phase lag to be compensated.

The steps involved in the Larsen and Swann method of PSS tuning are discussed below. Fig. 2.1 shows the simplified model of a single machine connected to an infinite bus [2]. The tuning procedure consists of the following steps:

1. Calculate the transfer function *GEP(s)* as shown in Fig. 2.1. [2]
2. Plot the phase lag of *GEP(s)* over the range of frequency of interest.
3. Tune the PSS as to provide suitable phase lead at this desired frequency.
4. Adjust the gain of the PSS (K_s) to one-third of the value that causes instability.

Note that the generator-exciter system in state space form is given by,

$$\dot{x} = A_{sys}x + B_{sys}u$$

$$y = C_{sys}x + D_{sys}u$$

$$y = \left[C_{sys}\left(sI - A_{sys}\right)^{-1}B_{sys} + D_{sys}\right]u$$

$$GEP(s) = \left[C_{sys}\left(sI - A_{sys}\right)^{-1}B_{sys} + D_{sys}\right]$$

where A_{sys}, B_{sys}, C_{sys} and D_{sys} are the system matrices.

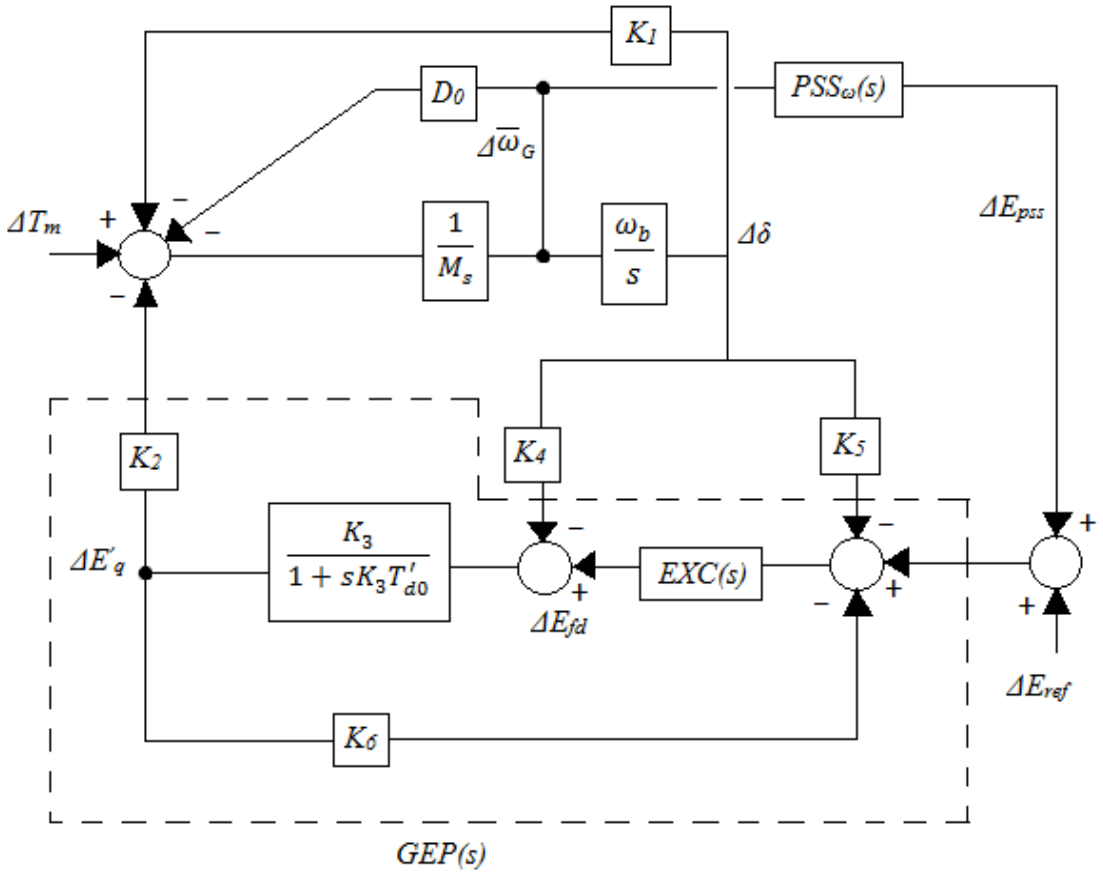

Fig 2.1 Simplified model of a single machine to an infinite bus

2.3 An example to demonstrate the Larsen and Swann method of PSS tuning

An example of the Larsen and Swann method is shown for reference. This example is applied to a small system. The dynamics of a simple two area power system shown in Fig 2.2 taken directly from [10] is to be improved. Each generator in the system is modeled with a fast response AC exciter. It is desired to add a PSS to each generator to improve the dynamic performance of the system.

The base case power flow solution of the two area system has a tie line power flow of 300 MW. The tie line power flow is increased by 50% to the steady state stability limit

of 376.7 MW, to 338.4 MW. The PSS at each generator is tuned using the Larsen and Swann method. The gain of all power system stabilizers is the same at all the four generators and is determined through eigenvalue analysis and time domain simulations.

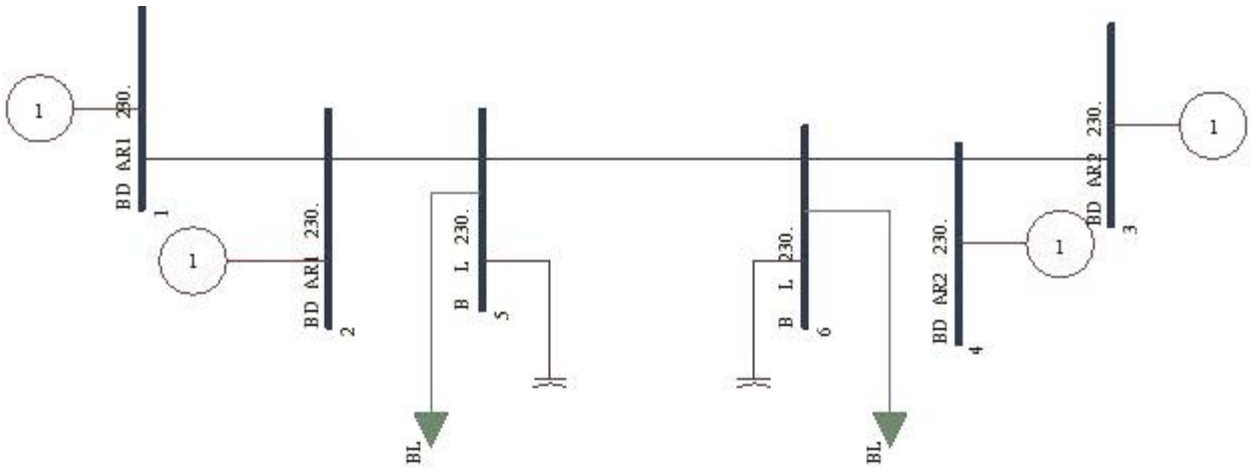

Fig 2.2 A two-area power system used as a test bed

For the example considered, the generators are modeled as model DG0S5 which represent the synchronous machine as a solid rotor generator, the exciter is modeled as the AC exciter (EXC30) [22].

The design steps for PSS design using the Larsen and Swann method are as follows:

1 Obtain System matrices A_{sys} , B_{sys} , C_{sys} , D_{sys} from power system simulation tools like DSA Tools.

2 Remove all the rows and columns due to rotor angles and speed and obtain *A', B', C', D'* matrices.

3 Form the overall system transfer function *GEP(s)*, draw the phase curve of *GEP(s)* – the ideal phase lead requirement by the PSS.

4 Choose PSS time constants to match the ideal curve over 0.1 to 2 Hz (the frequency range of interest for small signal stability). The PSS is forced to under compensate at frequencies below 1 Hz so that it does not reduce the synchronizing torque.

5 PSS gain is set using SSAT (complete eigenvalue analysis) and TSAT (time domain simulations).

2.3.1 Obtaining system state space representation (Matrices A_{sys}, B_{sys}, C_{sys}, D_{sys})

For each dynamic device, SSAT formulates the following model and uses it in all computations,

$$[\dot{x_d} = A_d x_d + B_d v_d + F_d u] \qquad (2.1)$$

$$[\dot{\iota_d} = C_d x_d + D_d v_d] \qquad (2.2)$$

where x_d is the n x 1 state vector for a device, v_d is the 2m x 1 voltage vector of voltages at the device terminal bus and any remote sensing buses, and i_d is the 2k x 1 currents injected into the network at the device terminals. If response computation is required and the input is specified as either V_{ref} in an exciter or P_{ref} in a governor, the input is contained in the vector u. For the system shown in Fig 2.2, the state variables for each generator-exciter system is given by the following equation

$$\left[x_d = \left(\omega, \delta, \psi_{fd}, \psi_{kd1}, \psi_{kq1}, \psi_{kq2}, x_{TF}, x_{TB}, x_{TA}\right)^T\right]. \qquad (2.3)$$

In DSA Tools, the generator states are placed before the exciter states for each machine in the vector of states. After running the complete eigenvalue analysis in SSAT, the overall system state matrix A_{sys} is computed from A_d, B_d, C_d, D_d and Y_n as,

$$\left[A_{sys} = A_d + B_d(Y_n - D_d)^{-1}C_d\right] \tag{2.4}$$

where,

$$A_d = \begin{bmatrix} A_{d1} & & \\ & \ddots & \\ & & A_{dn} \end{bmatrix} \qquad B_d = \begin{bmatrix} B_{d1} & & \\ & \ddots & \\ & & B_{dn} \end{bmatrix}$$

$$C_d = \begin{bmatrix} C_{d1} & & \\ & \ddots & \\ & & C_{dn} \end{bmatrix} \qquad D_d = \begin{bmatrix} D_{d1} & & \\ & \ddots & \\ & & D_{dn} \end{bmatrix}$$

and Y_n is the reduced network admittance matrix**.**

The complete system can be represented by the linearized set of Equations (2.5, 2.6) where input u is the exciter V_{ref} and the output y is the electrical torque T_e. The system matrices are obtained from SSAT. The details are as follows,

$$\left[\dot{x} = A_{sys}x + B_{sys}u\right] \tag{2.5}$$

$$\left[y = C_{sys}x + D_{sys}\right]. \tag{2.6}$$

For this system studied, the size of the A_{sys} matrix is 36 × 36; the size of the B_{sys} matrix is 36 × 4; and the size of the C_{sys} matrix is 4 × 36.

2.3.2 Estimation of generator-exciter transfer function

The rows and columns corresponding to the speed and rotor angle equations are removed from the A_{sys}, B_{sys}, C_{sys}, D_{sys} matrices to obtain the new state space representation *A', B', C', D'*.

The generator-exciter transfer function is obtained as

$$[GEP(s) = C'(sI - A')^{-1}B']. \quad (2.7)$$

2.3.3 Obtaining the generator-exciter phase plots for the two-area system in Fig 2.2

The phase angle lag of the generator-exciter system is plotted over the range of 0 to 2 Hz for each generator. The time constants of the PSS are found by curve fitting the PSS frequency response to the generator-exciter lag characteristic. The curve fitting process is biased to force the PSS to undercompensate at lower frequencies. The frequency responses for generators 1, 2, 3, and 4 in the two-area system can be seen in Fig 2.3, 2.4, 2.5, and 2.6 respectively.

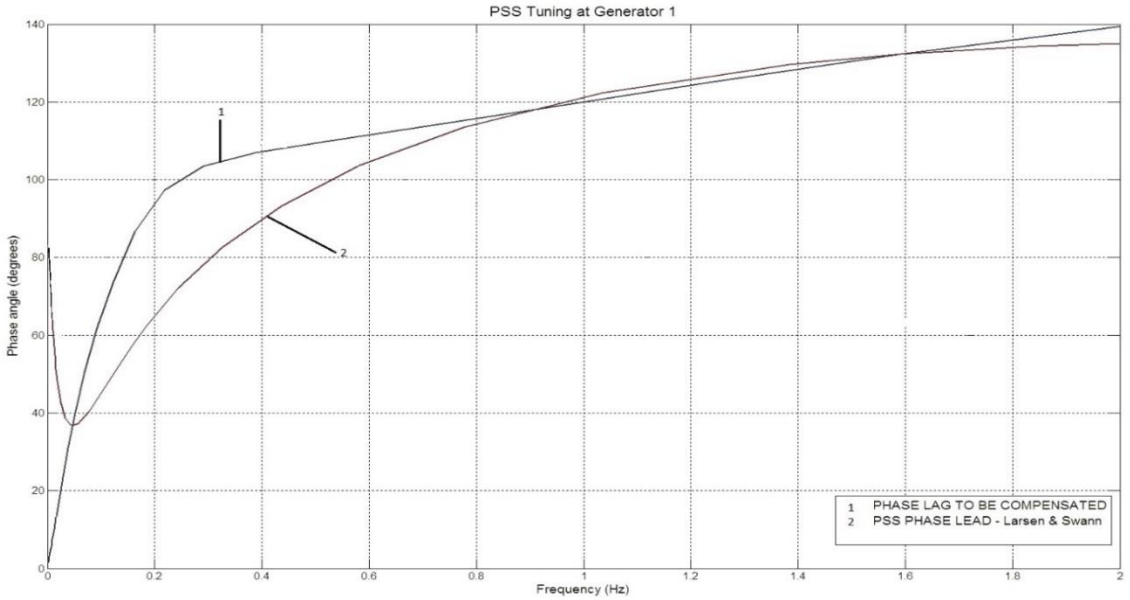

Fig 2.3 Generator-exciter 1 system frequency-phase plot for the two-area system in Section 2.3

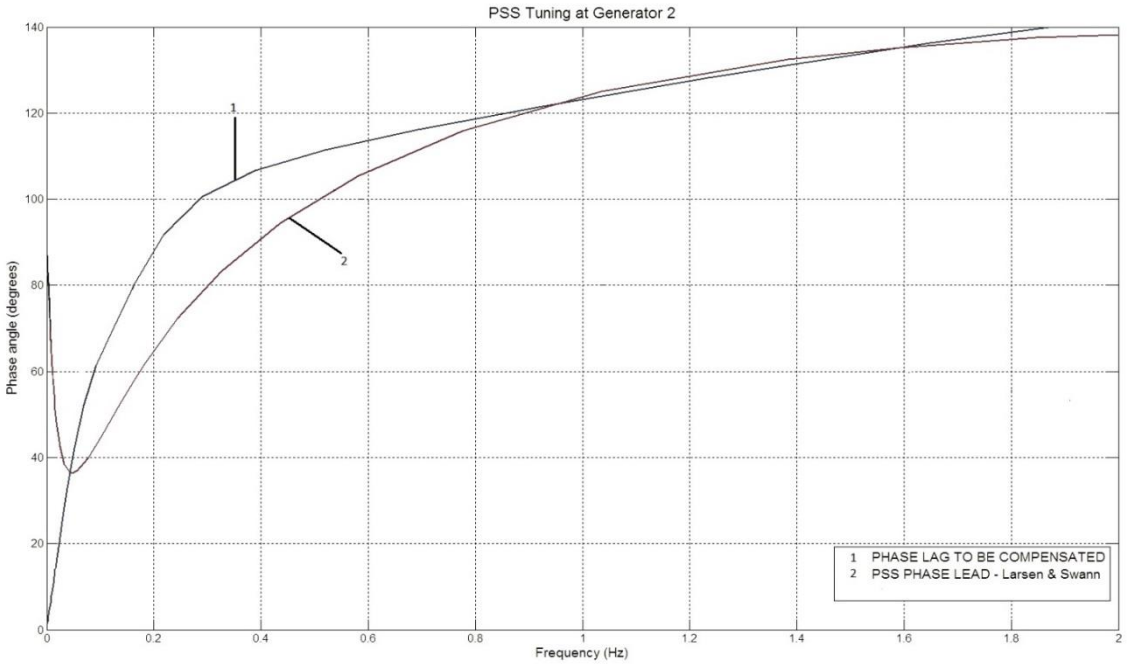

Fig 2.4 Generator-exciter 2 system frequency-phase plot for the two-area system in Section 2.3

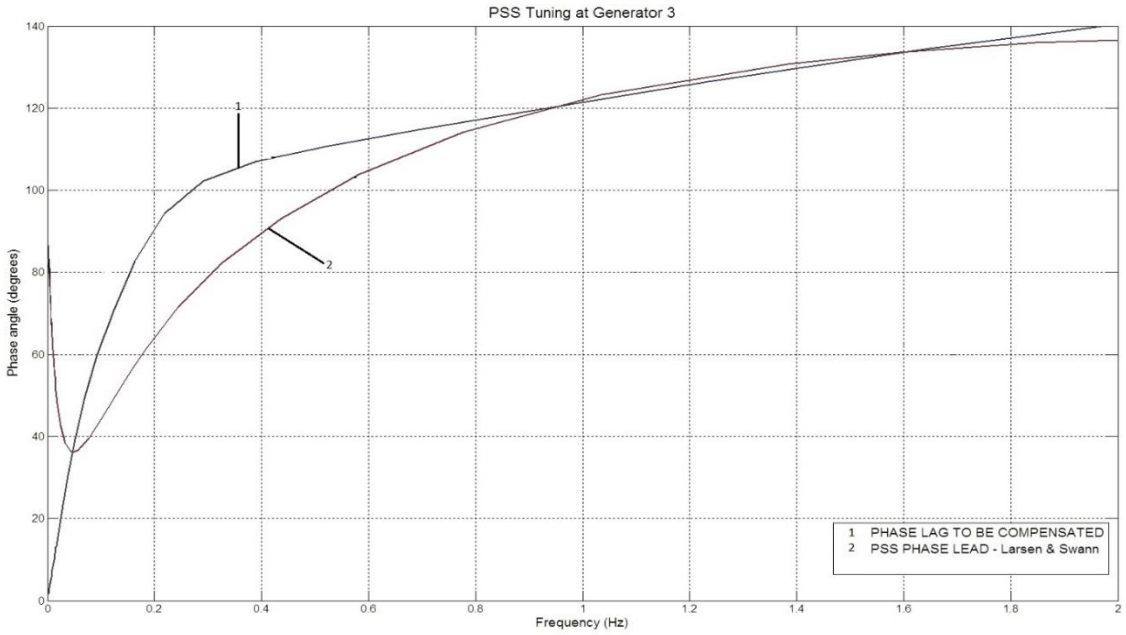

Fig 2.5 Generator-exciter 3 system frequency-phase plot for the two-area system in Section 2.3

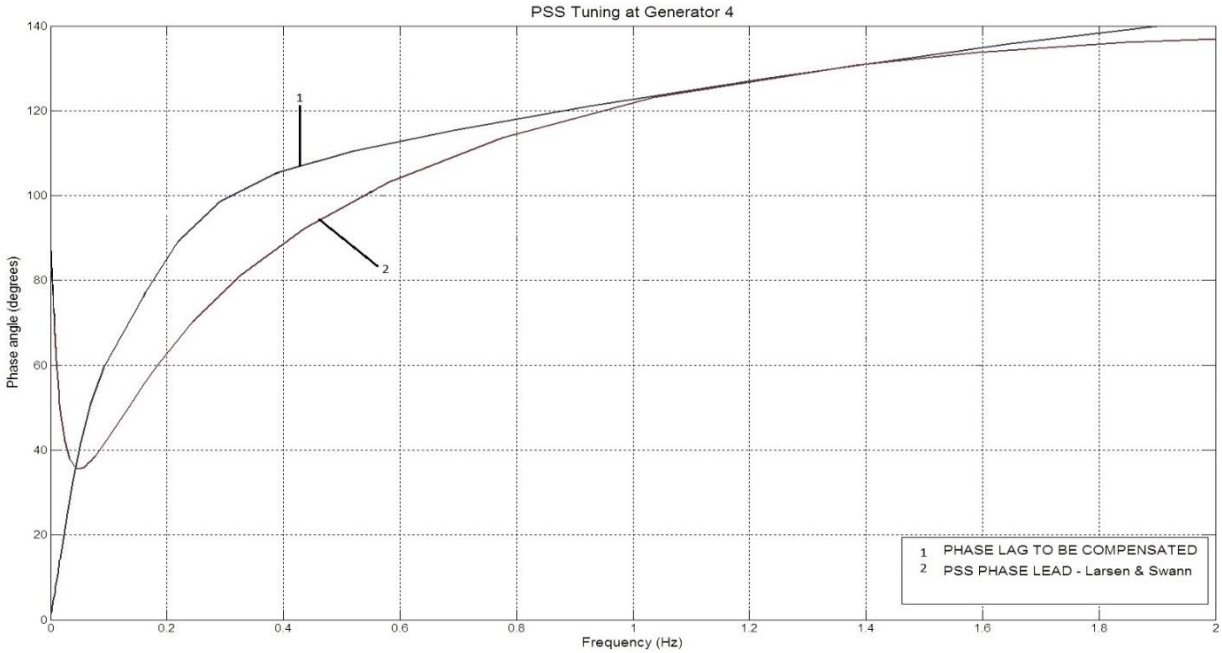

Fig 2.6 Generator-exciter 4 system frequency-phase plot for the two-area system in Section 2.3

2.3.4 Phase lead block design for the generator-exciter system in Section 2.3

The phase lag of the generator-exciter system in example in Section 2.3 has been evaluated. The phase lead blocks within the power system stabilizer model are determined by fitting the PSS lead characteristic to the generator-exciter lag. The power system stabilizer model (PSS1) [22] has the transfer function of the form in (2.8). The time constants for the PSS at each generator are listed in Table 2.1. The transfer function $G_s(s)$ is given by,

$$G_s(s) = \left(\frac{K_S T_5 s}{1 + T_5 s}\right)\left(\frac{1 + T_1 s}{1 + T_2 s}\right)\left(\frac{1 + T_3 s}{1 + T_4 s}\right) \tag{2.8}$$

where $T_1 - T_4$ are the lead/lag time constants (seconds) and T_5 is the washout time constant (seconds).

The MATLAB curve fitting tool is used for calculating the time constants T_1-T_4 of the PSS block. The curve fitting is modified such that the PSS undercompensates at lower frequency range. The function used for curve fitting to tune T_1-T_4 is,

$$\begin{aligned}\left[Y(X) = (180/\pi)\left(\frac{\pi}{2} - tan^{-1}(10X) + tan^{-1}(XT_1)\right.\right. \\ \left.\left. - tan^{-1}(XT_2) + tan^{-1}(XT_3) - tan^{-1}(XT_4)\right)\right]\end{aligned} \tag{2.9}$$

Table 2.1 PSS lead-lag parameters (seconds)

	PSS 1	**PSS 2**	**PSS 3**	**PSS 4**
T_1	0.9334	0.8919	0.8950	0.8513
T_2	0.0100	0.0100	0.0100	0.0100
T_3	0.1785	0.1920	0.1817	0.1823
T_4	0.0127	0.0100	0.0107	0.0100
T_5	10	10	10	10

2.3.5 Select PSS gain using eigenvalue analysis and time domain simulations

All the time constants for the PSS are now defined. The gain of the stabilizers still needs to be chosen. The gain of all the stabilizers will be held the same. Time domain simulations of a 6-cycle-duration three-phase fault in the middle of the tie line are conducted for different PSS gain. A good choice of gain for the stabilizers will provide sufficient damping torque to each generator in the system. The value of gain K_s is varied from 0 to 15. For each different gain, an eigenvalue analysis is also conducted to see the effect of the stabilizers on the critical mode. For PSS gains of 5, the system is underdamped. For gain K_s of 10 and 11, the system has acceptable overshoot and settling time. For gains of 15 and above, the system has prolonged overshoot and increased settling time. Table 2.2 shows the results obtained from eigenvalue analysis for exciter model EXC30.

Table 2.2 Results obtained from eigenvalue analysis for the exciter EXC30 in Section 2.3

No.	PSS Gain	Eigenvalue		Frequency (Hz)	Damping (%)	Critical Mode
		Real	Imaginary			
1	No PSS	-0.0631	2.3904	0.3804	2.64	Speed
Larsen and Swann Method						
2	5.0	-0.3004	2.4513	0.3901	12.16	Speed
3	10.0	-0.5210	2.5020	0.3982	20.38	Speed
4	11.0	-0.5628	2.5103	0.3995	21.88	Speed
5	15.0	-0.7250	2.5385	0.4040	27.46	Speed
6	20.0	-0.9139	2.5607	0.4076	33.61	Speed

Time domain simulations of the system in the example of Section 2.3 are conducted in TSAT. The power flow on the tie line in the two-area power system in the example is set to 338.46 MW. A three phase fault was applied at the middle of the tie line with a fixed clearing time of 6 cycles. The machine rotor angles are plotted for different values of PSS gain. The results of these simulations can be seen in Fig 2.7 to Fig 2.12. The Larsen and Swann method of PSS tuning for the two-area system studied in the example is implemented using a code in Matlab. The code for the same is attached in Appendix B.

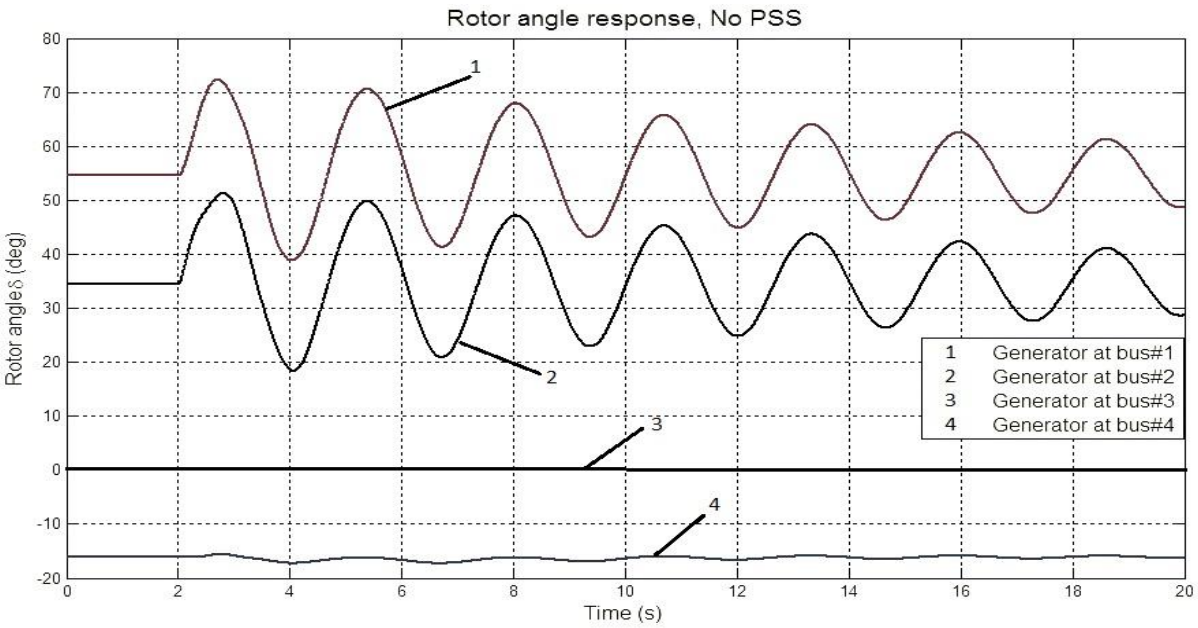

Fig 2.7 Rotor angle response with no PSS for the two-area power system in Section 2.3

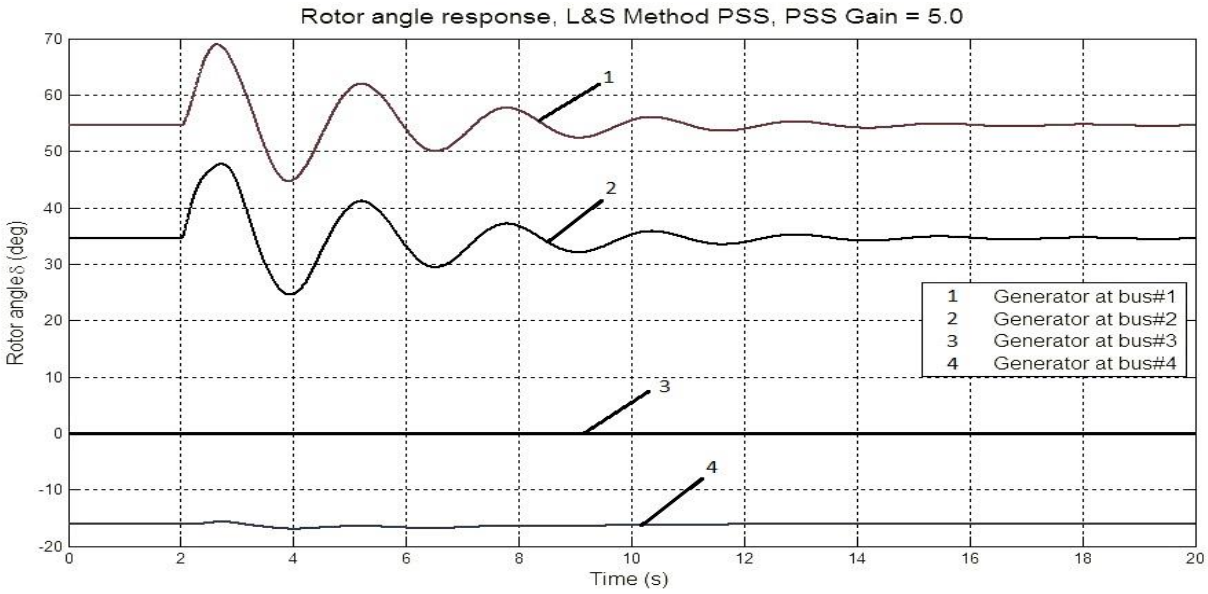

Fig 2.8 Rotor angle response with PSS Gain of 5.0 for the two-area power system in Section 2.3

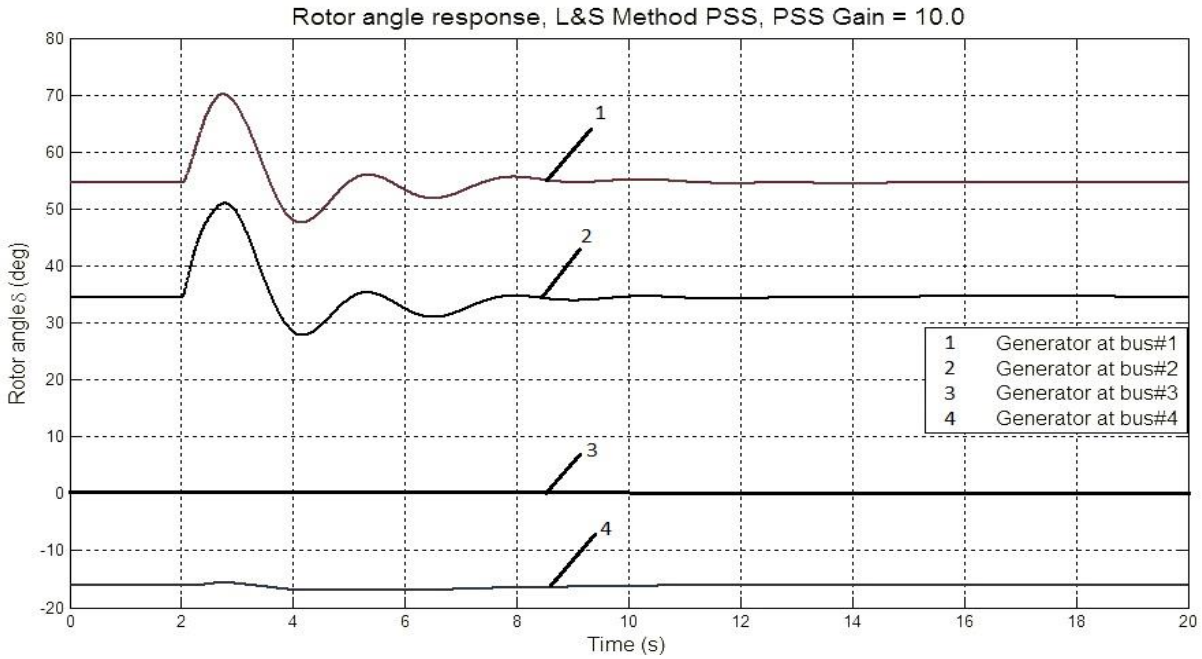

Fig 2.9 Rotor angle response with PSS gain of 10 for the two-area power system in Section 2.3

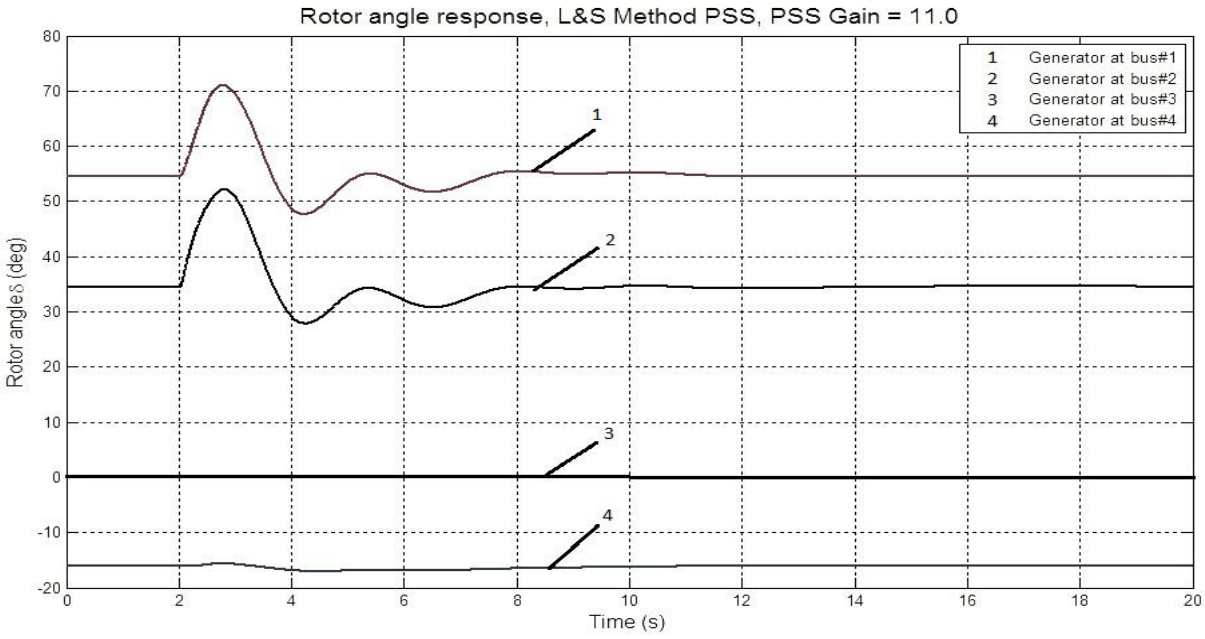

Fig 2.10 Rotor angle response with PSS gain of 11 for the two-area power system in Section 2.3

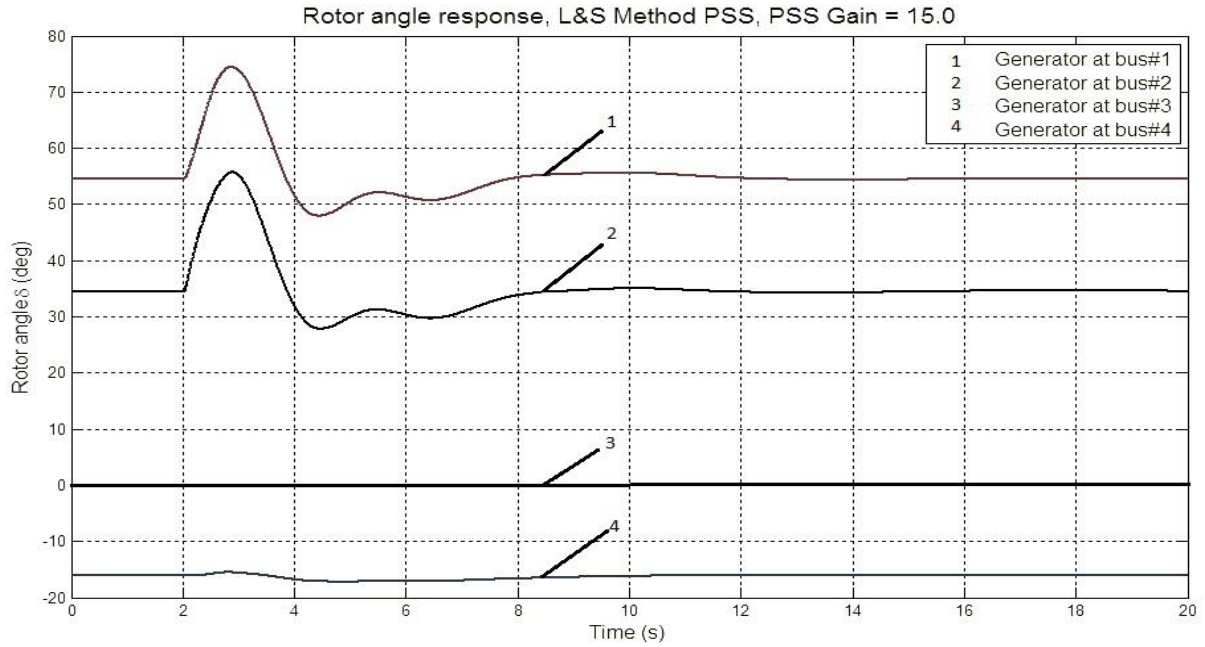

Fig 2.11 Rotor angle response with PSS gain of 15 for the two-area power system in Section 2.3

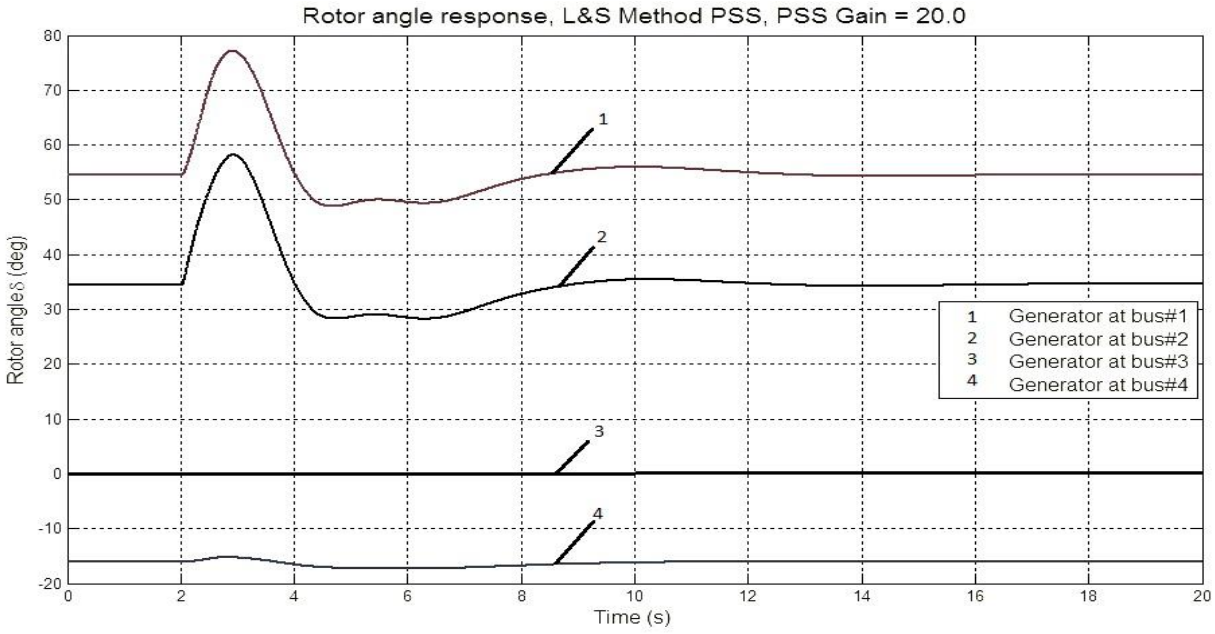

Fig 2.12 Rotor angle response with PSS gain of 20 for the two-area power system in Section 2.3.

2.4 Software limitations of the method

The actual power system data used as the test bed for the study is typical of the analysis data for a large system. Due to the large size of the system at hand and also the software limitations on the number of states, it is inconvenient to calculate the system matrices for the entire system. Hence, a method of PSS tuning different from the Larsen Swan algorithm is implemented. This alternative method is described in Chapter 3.

The SSAT DSA Tool [5] allows for eigenvalue analysis over a selected range of frequency and damping which gives the matrices for individual units. However, SSAT does not allow for complete eigenvalue analysis, since the number of states in the system exceeds the limit set by SSAT. As a result, the system matrices cannot be obtained.

CHAPTER 3 EXAMINATION OF OPERATING CONDITIONS WITH INCREASED SOLAR PENETRATION: SPRING 2010 LIGHT LOAD CASE

3.1 A test bed for an illustrative study

In order to assess the impact of high penetration of PV solar resources, operating data from the actual power system considered available for the spring 2010 light load case were used. These data exhibit the aforementioned high level of solar generation. In order to study this case, a commercial dynamic analysis software package was used to calculate power system dynamic models. In the study of small-signal power system dynamics, the time response of rotor angles of generators is characterized by *modes*. These modes may be oscillatory or completely damped. The critical modes are those with reduced damping. Reduced damping is particularly undesirable since the oscillations require longer time to decay. Such problematic modes are identified. The PSSs on the generators which participate in these dominant modes are then *retuned* to account for the changed operating conditions and improve the damping.

3.2 Description of the test: Spring 2010 light load case

For the spring 2010 light load data, a base case power flow is run and the local and inter-area modes are observed for frequency and damping. The base case is the case with zero solar PV generation. As the solar penetration level is added and the PV generation is increased, the effects on damping show that damping is reduced and modal frequencies are approximately unchanged. The solar PV penetration is added in steps of 10% up to 50% in order to assess the impact on system dynamics. The 30%, 40% and 50% penetration levels

show significantly lowered damping of the critical modes. In depth analyses of the area, the type of plant, and the generators are conducted corresponding to the dominant modes.

3.3 Base case scenario: Spring 2010 light load case

The base case (with no PV penetration) is considered and eigenvalue analysis is carried out using the SSAT DSA tool [5] to check the frequency and damping of the identified critical modes. These are standard software tools that are widely used in the electric power industry. For the base case, the eigenvalues associated with the dominant modes are shown in Table 3.1. Note that damping is represented as a percentage and as a positive number *D*.

Table 3.1 Base case dominant modes: Spring 2010 light load case

Mode number	**Eigenvalue**		***f (Hz)***	**Damping** ***D (%)***	**Dominant state**
	Real	**Imaginary**			
14	-2.4105	20.9021	3.3267	11.46	Angle
15	-2.436	19.7426	3.1421	12.25	Angle
90	-0.908	22.0733	3.5131	4.11	Speed
91	-0.6759	20.4277	3.2512	3.31	Speed
88	-0.7957	18.8228	2.9958	4.22	Speed
88	-1.0736	21.2937	3.389	5.04	Speed
89	-0.8275	19.152	3.0481	4.32	Speed
89	-1.0736	21.2937	3.389	5.04	Speed

3.4 Solar PV penetration set at 10% and 20%

The described test bed was also studied with PV generation added. For example, 10% of the total name plate generation was supplied by PV and in turn, some conventional generators were shut down in order to account for this additional generation. Similar steps were carried out for the 20% case. The results are produced in Tables 3.2 and 3.3.

It is observed that the 10% and 20% PV generation cases did not impact damping. Hence these cases are not considered for further analysis. Different scenarios were then studied where specific generators were switched off to allow for the high PV generation.

Table 3.2 Dominant modes for the 10% PV generation case: Spring 2010 light load case

Mode number	**Eigenvalue**		***f (Hz)***	**Damping** ***D (%)***	**Dominant state**
	Real	**Imaginary**			
14	-2.4027	20.8901	3.3248	11.43	Angle
15	-2.4204	19.7196	3.1385	12.18	Angle
91	-0.7527	21.2089	3.3755	3.55	Speed
88	-0.8806	18.488	2.9425	4.76	Angle
88	-1.1691	20.7993	3.3103	5.61	Speed
89	-0.9133	18.7964	2.9916	4.85	Speed
89	-1.1691	20.7993	3.3103	5.61	Angle

Table 3.3 Dominant modes for the 20% PV generation case: Spring 2010 light load case

Mode Number	Eigenvalue		*f* (Hz)	Damping *D* (%)	Dominant State
	Real	Imaginary			
14	-2.3676	19.8119	3.1532	11.87	Angle
88	-0.9353	18.2836	2.9099	5.11	Angle
88	-1.2322	20.509	3.2641	6	Speed
89	-0.97	18.5842	2.9578	5.21	Speed
89	-1.2322	20.509	3.2641	6	Speed

3.5 Generators shut down to allow for the excess PV penetration

As PV generation is added and increased from 30% to 50%, conventional generators are shut down to allow for the PV generation. The generators shut down for this task were decided depending on the type of generating units and the amount of generation.

3.5.1 Shutting down the CT and GT units to accommodate PV generation

A test was done to evaluate the reduction of combustion turbine (CT) and gas turbine (GT) generation. This task deals with altering the economic generation scheduling. Since the GT and CT units have relatively high operating costs, these types of conventional generator units are shut down to account for the additional PV generation. The PV is added in varying amounts (30%, 40%, and 50%) and equal amounts of generation are backed off

from conventional generators. The generators that are selected to be shut down belong to the CT and GT type. The results are shown in Table 3.4.

3.5.2 Shutting down an aging coal unit

In simulation, the generating units at an aging coal generation station are shut down in order to account for the additional PV generation. The results are shown in Table 3.5.

3.5.3 Shutting down alternative aging coal units

Alternative aging coal units in the area under study are shut down in simulation in order to account for the additional PV generation. The results are shown in Table 3.6.

Table 3.4 Comparison between 30%, 40% and 50% PV penetration cases when CT and GT units are switched off: Spring 2010 light load case

Dominant state	**Base case**		**30% PV**		**40% PV**		**50% PV**	
Bus	***f*** **(Hz)**	***D*** **(%)**	***f*** **(Hz)**	***D*** **(%)**	***f*** **(Hz)**	***D*** **(%)**	***f*** **(Hz)**	***D*** **(%)**
14	3.33	11.46	3.32	11.38	3.32	11.43	3.32	11..42
15	3.14	12.25	3.12	12.18	3.12	12.22	3.12	12.23
90	3.51	4.11	3.51	4.12	3.51	4.43	3.50	4.45
91	3.25	3.31	3.26	3.31	3.24	3.34	3.51	2.61
88	3.04	4.32	2.91	5.01	2.98	4.3	3.00	4
88	3.39	5.04	3.27	5.9	3.36	5.15	3.41	4.84
89	2.99	4.22	2.96	5.12	3.03	4.42	3.06	4.13
89	3.39	5.04	3.27	5.9	3.36	5.15	3.41	4.84

Table 3.5 Comparison between 30%, 40% and 50% PV cases when aging coal units are switched off: Spring 2010 light load case

Dominant state	**Base case**		**30% PV**		**40% PV**		**50% PV**	
Bus	***f*** ***(Hz)***	***D*** ***(%)***	***f*** ***(Hz)***	***D*** ***(%)***	***f*** ***(Hz)***	***D*** ***(%)***	***f*** ***(Hz)***	***D*** ***(%)***
88	2.99	4.22	2.91	5.09	2.97	4.4	3.01	4
88	3.39	5.04	3.27	5.98	3.36	5.25	3.41	4.83
89	3.05	4.32	2.96	5.19	3.03	4.51	3.06	4.13
89	3.9	5.04	3.27	5.98	3.36	5.25	3.41	4.83

Table 3.6 Comparison between 30%, 40% and 50% PV cases when alternative aging coal units are switched off: Spring 2010 light load case

Dominant state	**Base case**		**30% PV**		**40% PV**		**50% PV**	
Bus	***F*** ***(Hz)***	***D*** ***(%)***	***f*** ***(Hz)***	***D*** ***(%)***	***f*** ***(Hz)***	***D*** ***(%)***	***f*** ***(Hz)***	***D*** ***(%)***
90	3.51	4.11	3.55	4.04	3.51	4.35	3.50	4.49
91	3.25	3.31	3.25	3.25	3.24	3.3	3.19	2.8
88	2.99	4.22	2.90	5.2	2.96	4.48	3.01	3.99
88	3.39	5.04	3.25	6.1	3.34	5.34	3.41	4.83
89	3.05	4.32	2.95	5.31	3.02	4.6	3.07	4.12
89	3.39	5.04	3.25	6.1	3.35	5.34	3.42	4.83

3.6 Time domain analysis

The 50% PV penetration case with the CT and GT units turned off (Table 3.4) shows the lowest damping for the dominant mode at a specific system generation bus 91. This case is considered for further analysis. Time domain analysis is conducted using the TSAT. A three-phase fault is created on the bus which is electrically closest to bus 91 since such a fault affects the critically damped modes the most. The fault is cleared after 6 cycles. The behavior of the generator at bus 91 is monitored and generator speed is plotted in Fig. 3.1. Further, Prony analysis is conducted to validate the results and the dominant modes are shown in Table 3.7.

3.7 Prony analysis

Prony analysis is a feature of the TSAT DSA tool and is used in time-domain simulations. Prony analysis is a methodology that extends Fourier analysis by directly

estimating the frequency, damping strength and relative phase of the modal components present in a given signal [12]. The ability to extract such information from transient stability program simulations and from large scale system tests or disturbances could provide:

- Parametric summaries for damping studies (data compression)
- Quantified information for adjusting remedial controls (sensitivity analysis and performance evaluation)
- Insight into modal interaction mechanisms (modal analysis)
- Reduced simulation times for damping evaluation (prediction).

A linear, time-invariant dynamic system is brought to an initial state $x(t_0) = x_0$ at time t_0. This is done by introducing a test input or disturbance. If the input is removed without any subsequent inputs or disturbances, the system state will 'ring down' according to a linearized differential equation of the form

$$\dot{x} = Ax$$

where x is the state of the system and n is the order of the system. The solution to the above equation is expressed in terms of the eigenvalues, right eigenvectors and left eigenvectors of matrix A.

The strategy for obtaining Prony solution is summarized as follows:

1. Construct a discrete linear prediction model that fits the record.
2. Find the roots of the characteristic polynomial associated with the linear prediction model.

3. Using the roots as the complex modal frequencies for the signal, determine the amplitude and initial phase for each mode.

These steps are performed in *z*-domain. For power system application, the eigenvalues would be translated to *s*-domain. Prony's main contribution is at step 1.

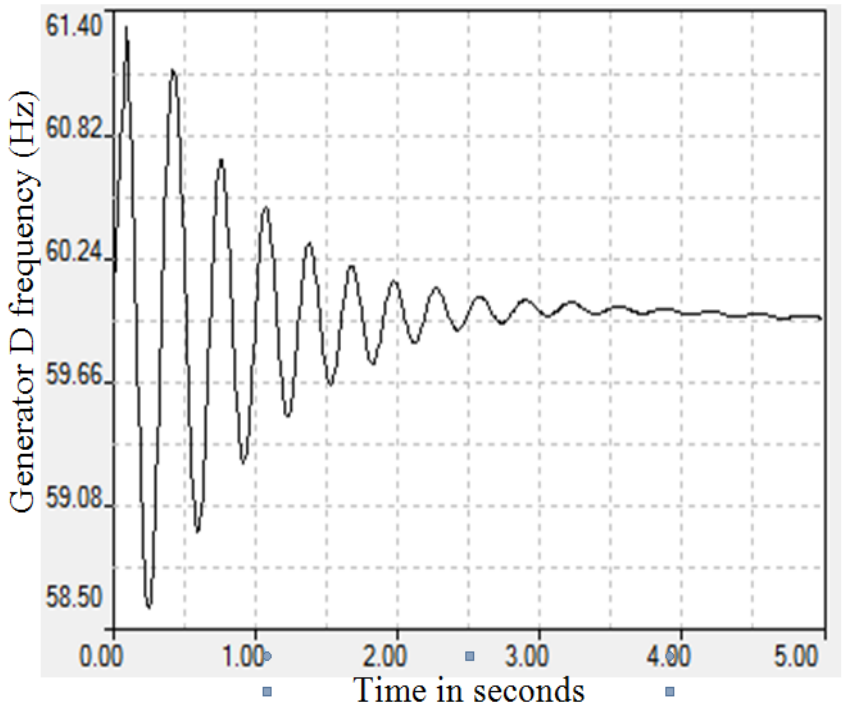

Fig 3.1 Generator 91 speed plot with the original PSS settings: Spring 2010 light load case

The time domain simulation are carried out as defined in test 5 (Appendix A) and the results are shown in Table 3.7 identify the poorly damped mode of oscillation (mode 6). This result is consistent with the result produced in Table 3.4 that identifies the mode associated with the dominant state at generation bus 91. The critical mode has a frequency of 3.51 Hz and damping of 2.61%.

Table 3.7 Time domain results: Spring 2010 light load case

Mode number	***f*** **(Hz)**	***D*** **(%)**
1	21.684	41.954
2	13.238	52.599
3	30.25	33.573
4	2.97	14.357
5	1.213	69.4
6	3.342	2.868
7	9.00	16.784

3.8 Power system stabilizer tuning

Due to the limitations in the implementation of the Larsen and Swann method for PSS tuning, this method cannot be used to retune the PSSs existing on the identified conventional generators. Another method of PSS retuning is adopted. The modes corresponding to buses 90 and 91 have to be retuned simultaneously since retuning the mode with the critically low damping caused the damping of the other mode to reduce. This method is based on the procedure described in reference [9]. The steps involved are as below,

1. Using SSAT, the frequency response of the transfer function for the dominant mode at bus 91 without the PSS is plotted in Fig 3.2. This was done because the system size does not allow the direct calculation of the system matrices.
2. At the frequency of the mode at 3.51 Hz, the corresponding phase lag of 136.4 degrees is obtained.

3. The data from the SSAT is used to plot the frequency response in MATLAB.
4. For the above phase lag, the lead / lag time constants T_1, T_2, T_3, T_4 are calculated using a MATLAB code for PSS design using,

$$f = 3.51$$
$$\omega = 2\pi f$$
$$\theta = \frac{-136.4\pi}{180 \times 2}$$
$$\alpha = \frac{(1 + \sin\theta)}{(1 - \sin\theta)}$$
$$\tau = \frac{1}{\omega\sqrt{\alpha}}$$

with α and τ being the lead / lag time constants, and these expressions are in Hz, r/s, radians and seconds.

5. Similar steps were carried out for the dominant mode at bus 90 for a phase lag of 96.5 degrees.

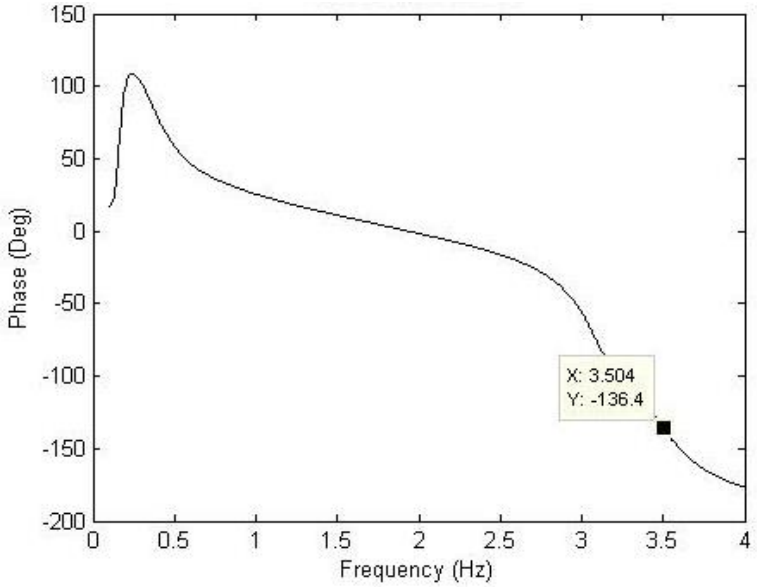

Fig 3.2 Frequency response of the 91 generator-exciter transfer function: Spring 2010 light load case

3.9 Results of PSS retuning

After the retuning process, the new values of time constants obtained are then fed into the dynamic data file in SSAT. The time constants before and after retuning are shown in Table 3.8.

Table 3.8 Original and new values of PSS lead/lag time constants: Spring 2010 light load case

Dominant generator modes	T_1	T_2	T_3	T_4
	(seconds)			
90	0.6	0.07	0.6	0.07
91	0.6	0.07	0.6	0.07
New values for PSS retuning				
90	0.0371	0.2358	0.0371	0.2358
91	0.1454	0.1191	0.1454	0.1191

The T_1-T_4 time constants for the standard IEEE- PSS model [11] were modified in the retuned PSS and the eigenvalue analysis is once again carried out using SSAT. The new results were compared with the original results and are shown in Table 3.9.

Table 3.9 Improvement in damping of the identified modes on retuning the PSS: spring 2010 light load case

Dominant generator modes	**50% PV case**			
	Original PSS settings		**Retuned PSS**	
	***f* (Hz)**	***D* (%)**	***f* (Hz)**	***D* (%)**
90	3.50	4.45	3.4121	7.38
91	3.51	2.61	3.1179	5.90

Thus, the critically low damping of 2.61% is improved to 5.9% and that of 4.45% is improved to 7.38%. The result is verified through time domain simulation which is explained in 3.6. Fig. 3.3 shows the generator speed plot with the retuned PSS. Prony Analysis is conducted to validate the new results obtained and the dominant modes are shown in Table 3.10.

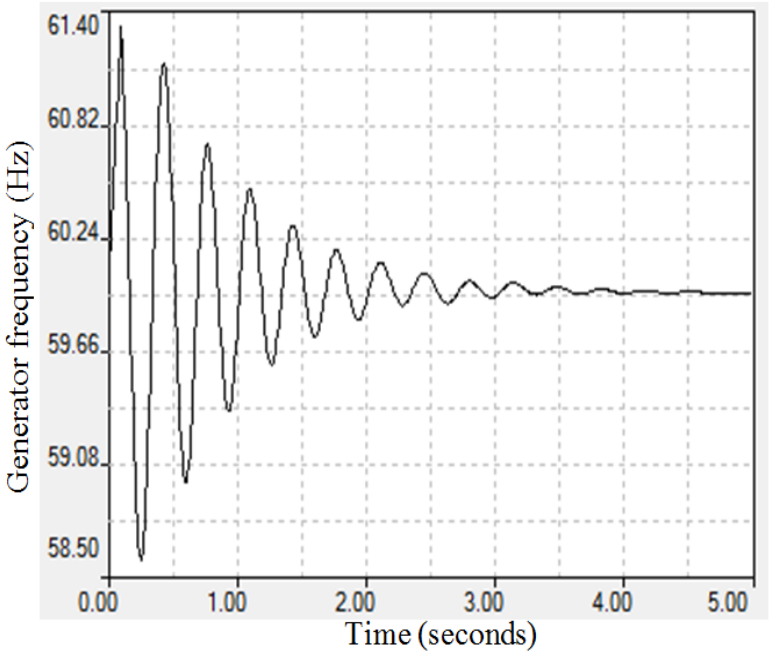

Fig 3.3 Generator 91 speed plot with the new PSS settings

The time domain simulation results in Table 3.10 identify the poorly damped mode whose damping has improved due to PSS retuning (mode 6) from 2.868% to 6.907%. This result is consistent with the result produced in Table 3.9 that identifies the mode associated with the dominant state at bus 91. That mode has a frequency of 3.1179 Hz and a damping of 5.9%. Fig. 3.4 shows the improvement in damping of the oscillations with the new PSS settings compared to the original settings. The transient observed in Fig 3.4 occurs due to Test 5 (see Appendix A).

Table 3.10 Time domain results: Spring 2010 light load case

Mode number	***f (Hz)***	***D (%)***
1	60.5	19.602
2	51.339	21.703
3	60.5	20.78
4	42.468	24.274
5	33.593	26.841
6	2.966	6.907
7	25.001	29.271
8	11.923	45.696
9	18.833	32.595
10	2.140	31.058
11	3.552	10.941
12	5.962	7.818

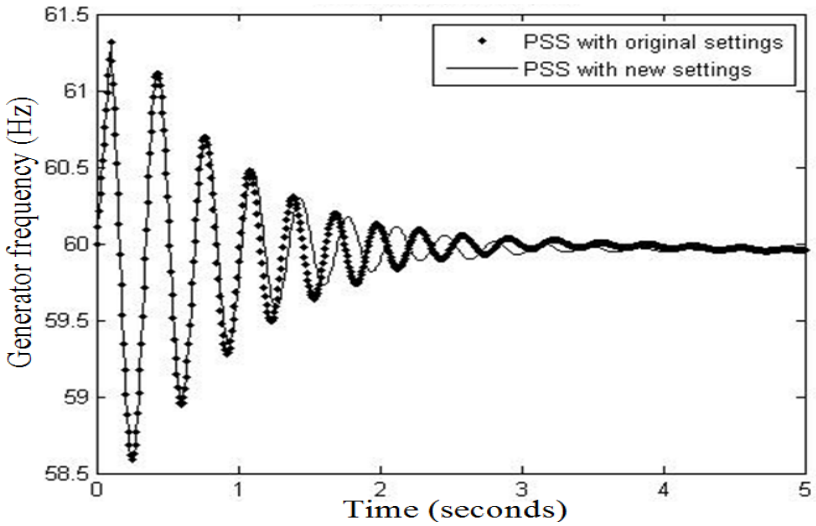

Fig 3.4 Comparison between the 91 generator speed with original and new PSS settings: Spring 2010 light load case

The impact of PV penetration on selected buses is observed. Eigenvalue analysis is carried out and reduction in damping performance is observed. Time domain simulations (test 5 – Appendix A) are also performed to see the oscillations which take longer time to damp. The PSS existing on the generators observed are retuned to damp the oscillations faster. The improvement in damping is observed graphically as the generator speed is plotted for the case where the PSS is at the original setting and the case where the PSS is retuned.

CHAPTER 4 EXAMINATION OF OPERATING CONDITIONS WITH INCREASED SOLAR PENETRATION: SUMMER 2018 PEAK LOAD CASE

4.1 A test bed for an illustrative study

In order to assess the impact of high penetration of PV solar resources, operating data from the actual power system considered for the summer 2018 peak load case were used. These data exhibit the aforementioned high level of solar generation. In order to study this case, the commercial dynamic software package used to study summer 2018 peak load data was used to calculate power system dynamic models. In the study of small-signal power system dynamics, the time response of rotor angles of generators, characterized by *modes*, may be oscillatory or completely damped. The critical modes are those with reduced damping. Reduced damping is particularly undesirable since the oscillations require longer time to decay. Such problematic modes are identified. The PSSs on the generators which participate in these dominant modes are then *retuned* to account for the changed operating conditions and improve the damping.

4.2 Description of the test: Summer 2018 peak load case

For the summer 2018 peak load data, a base case power flow is run and the local and inter-area modes are observed for frequency and damping. The base has zero solar PV generation. As the solar penetration level is added and the PV generation is increased, the effects on damping show that damping is reduced and modal frequencies are approximately unchanged. The solar PV penetration is added in steps of 10% up to 50% in order to assess the impact on system dynamics. The damping of the critical modes is lowered as the

penetration of PV generation is increased up to 50%. In depth analyses of the area, the type of plant, and the generators are conducted corresponding to the dominant modes.

4.3 Base case scenario: Summer 2018 peak load case

The steps followed are similar to the steps followed for the assessment of the spring light load case. The base case (with zero PV penetration) is considered and eigenvalue analysis is carried out using the SSAT DSA tool to check the frequency and damping of the identified critical modes. For the base case, the eigenvalues associated with the dominant modes are shown in Table 4.1. Damping is represented as a percentage and as a positive number *D*.

Table 4.1 Base case dominant modes: Summer 2018 peak load case

Mode number	**Eigenvalue**		***f (Hz)***	**Damping** ***D (%)***	**Dominant state**
	Real	**Imaginary**			
93	-0.7971	18.7865	3.0754	1.81	Speed
94	-1.5115	20.8487	3.4336	3.65	Speed
95	-1.0169	18.4465	3.0625	2.37	Speed
96	-1.4946	20.7996	3.4107	4.42	Angle
97	-0.997	18.4594	3.0477	2.85	Speed
98	-1.4801	20.8878	3.4424	3.46	Speed
99	-1.5224	18.2267	3.0699	2.03	Speed

4.4 Generators shut down to allow for the excess PV penetration

As PV generation is added and increased from 10% to 50%, conventional generators are shut down to allow for the PV generation. The generators shut down for this task were decided depending on the type of generating units and the amount of generation.

- Shutting down the CT and GT units

This is carried out on the steps of Test 1 (see Appendix A). The PV is added in increasing amounts (10%, 20%, 30%, 40% and 50%) and equal amounts of generation are backed off from conventional generators. The generators that are selected to be shut down belong to the CT and GT type. The results are shown in Table 4.2.

Table 4.2 Comparison between 10%, 20%, 30%, 40% and 50% PV penetration cases when CT and GT units are switched off (test 1)

Dominant state	**Base case**		**10%**		**20%**		**30%**		**40%**		**50%**	
Bus	***f*** **(Hz)**	***D*** **(%)**	***f*** **(Hz)**	***D*** **(%)**	***f*** **(Hz)**	***D*** **(%)**	***f*** **(Hz)**	***D*** **(%)**	***f*** **(Hz)**	***D*** **(%)**	***f*** **(Hz)**	***D*** **(%)**
93	3.08	1.81	3.08	1.78	3.08	1.73	3.09	1.65	3.09	1.59	3.09	1.58
94	3.43	3.65	3.44	3.61	3.44	3.54	3.44	3.42	3.44	3.33	3.44	3.32
95	3.06	2.37	3.06	2.34	3.07	2.28	3.07	2.19	3.08	2.13	3.08	2.11
96	3.41	4.42	3.41	4.37	3.41	4.3	3.42	4.17	3.42	4.07	3.42	4.05
97	3.05	2.85	3.05	2.82	3.05	2.76	3.06	2.67	3.06	2.59	3.06	2.58
98	3.44	3.46	3.44	3.42	3.45	3.35	3.45	3.23	3.45	3.14	3.45	3.12

From Table 4.2 it is observed that the damping consistently decreases as the PV generation is increased. Carrying out Tests 1, 2 and 3 (see Appendix A) showed the same results as obtained in Table 4.2.

4.5 Time domain analysis

The varying PV penetration cases with the CT and GT units turned off (Table 4.2) show the lowering of damping for the dominant modes at specific system generation buses. Buses 93 to 98 showed critically low damping as the PV generation was increased. These cases are considered for further analysis. Time domain analysis is conducted using the TSAT (see Appendix A for test 5). A three-phase fault is created on bus which is electrically closest to the identified buses since such a fault affects the critically damped modes the most. The fault is cleared after 6 cycles. The behavior of the generators at these buses is monitored and Prony analysis is conducted to validate the results and the dominant modes are shown in Tables 4.3 - 4.7.

Table 4.3 Time domain results for 10% PV penetration case: Summer 2018 peak load case

Mode number	***f*** **(Hz)**	***D*** **(%)**
1	3.03	3.96
2	3.44	4.61
3	3.01	3.566
4	3.4	5.243
5	3.09	3.687
6	3.48	2.374

Table 4.4 Time domain results for 20% PV penetration case: Summer 2018 peak load case

Mode number	f **(Hz)**	D **(%)**
1	3.03	4.517
2	3.44	3.549
3	3.02	3.616
4	3.37	6.25
5	3.08	3.257
6	3.47	4.145

Table 4.5 Time domain results for 30% PV penetration case: Summer 2018 peak load case

Mode number	f **(Hz)**	D **(%)**
1	3.03	3.88
2	3.42	6.82
3	2.88	3.572
4	3.35	6.737
5	3.12	4.012
6	3.47	3.909

Table 4.6 Time domain results for 40% PV penetration case: Summer 2018 peak load case

Mode number	***f*** **(Hz)**	***D*** **(%)**
1	2.92	1.017
2	3.52	4.83
3	2.73	1.808
4	3.47	4.145
5	3.09	4.043
6	3.51	5.623

Table 4.7 Time domain results for 50% PV penetration case: Summer 2018 peak load case

Mode number	***f*** **(Hz)**	***D*** **(%)**
1	3.19	4.414
2	3.45	3.31
3	3.26	3.341
4	3.38	4.998
5	3.18	1.444
6	3.49	4.248

The Prony analysis results demonstrate the same trend with the reduction of the damping as shown by the eigenvalue analysis results

4.6 Steps carried out in retuning the PSS

Task 4 gives the steps to obtain the lead / lag time constants of each power system stabilizer depending on the phase lag to be compensated by the PSS (see Appendix A). For

frequency of each mode, corresponding phase lag was obtained from frequency response of the excitation system transfer function. Table 4.8 shows the original and the new values of time constants obtained. Using these new values, the PSS were retuned and improvement in damping performance is shown in Table 4.9.

Table 4.8 Original and new values of PSS lead/lag time constants: Summer 2018 peak load case

Dominant generator modes	T_1	T_2	T_3	T_4
	(seconds)			
93	0.6	0.07	0.6	0.07
94	0.6	0.07	0.6	0.07
95	0.6	0.07	0.6	0.07
96	0.6	0.07	0.6	0.07
97	0.6	0.07	0.6	0.07
98	0.6	0.07	0.6	0.07
New values for PSS retuning				
93	0.1249	0.1457	0.1249	0.1457
94	0.0278	0.2770	0.0278	0.2770
95	0.1124	0.1539	0.1124	0.1539
96	0.3739	0.0936	0.3739	0.0936
97	0.1324	0.1428	0.1324	0.1428
98	0.0266	0.2824	0.0266	0.2824

The improvement in damping of the oscillations for the dominant modes at generators 93 to 98 is observed in TSAT. The damping of oscillations for these modes with original PSS settings and new PSS settings are plotted and compared. Figures 4.1 – 4.6 show

the improvement in the damping performance for these modes (93 – 98) after retuning each PSS.

Table 4.9 Improvement in damping of the identified modes on retuning the PSS: Summer 2018 peak load case

Dominant state	**Base case**		**10%**		**20%**		**30%**		**40%**		**50%**	
Bus	***f*** **(Hz)**	***D*** **(%)**	***f*** **(Hz)**	***D*** **(%)**	***f*** **(Hz)**	***D*** **(%)**	***f*** **(Hz)**	***D*** **(%)**	***f*** **(Hz)**	***D*** **(%)**	***f*** **(Hz)**	***D*** **(%)**
93	3.08	1.81	2.99	4.24	2.9929	4.22	2.9979	4.19	3.002	4.16	3.002	4.16
94	3.43	3.65	3.318	7.23	3.3191	7.2	3.321	7.16	3.323	7.12	3.323	7.11
95	3.06	2.37	2.936	5.5	2.938	5.49	2.943	5.46	2.946	5.44	2.946	5.44
96	3.41	4.42	3.31	7.17	3.311	7.13	3.314	7.07	3.315	7.01	3.316	7.00
97	3.05	2.85	2.938	5.39	2.94	5.38	2.945	5.34	2.948	5.32	2.948	5.31
98	3.44	3.46	3.324	7.07	3.325	7.04	3.327	6.99	3.329	6.95	3.329	6.94

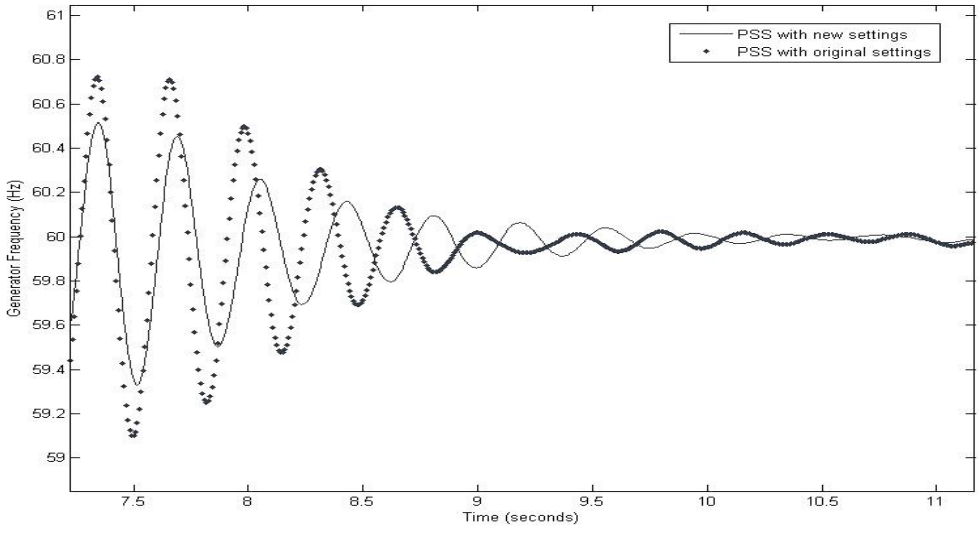

Fig 4.1 Comparison between the 93 generator speed with original and new PSS settings: Summer 2018 peak load case

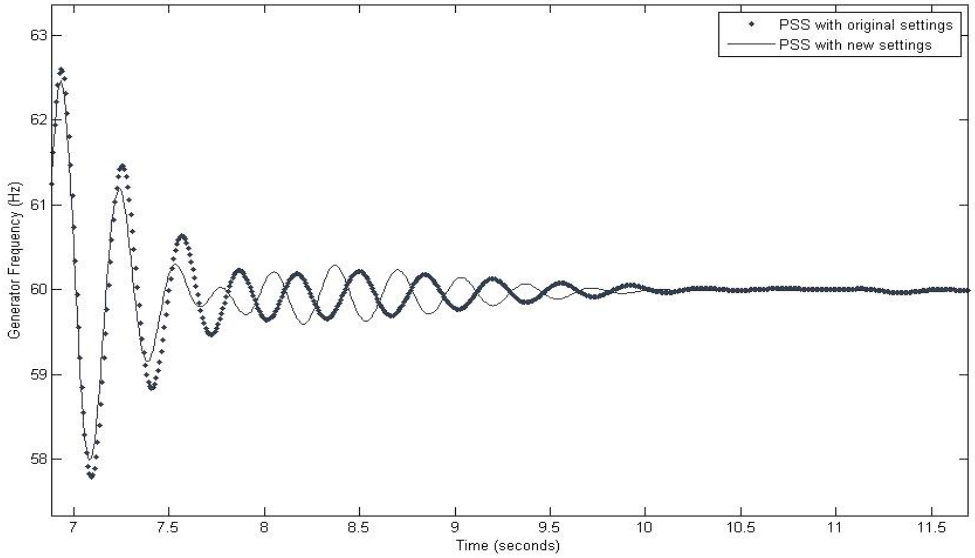

Fig 4.2 Comparison between the 94 generator speed with original and new PSS settings: Summer 2018 peak load case

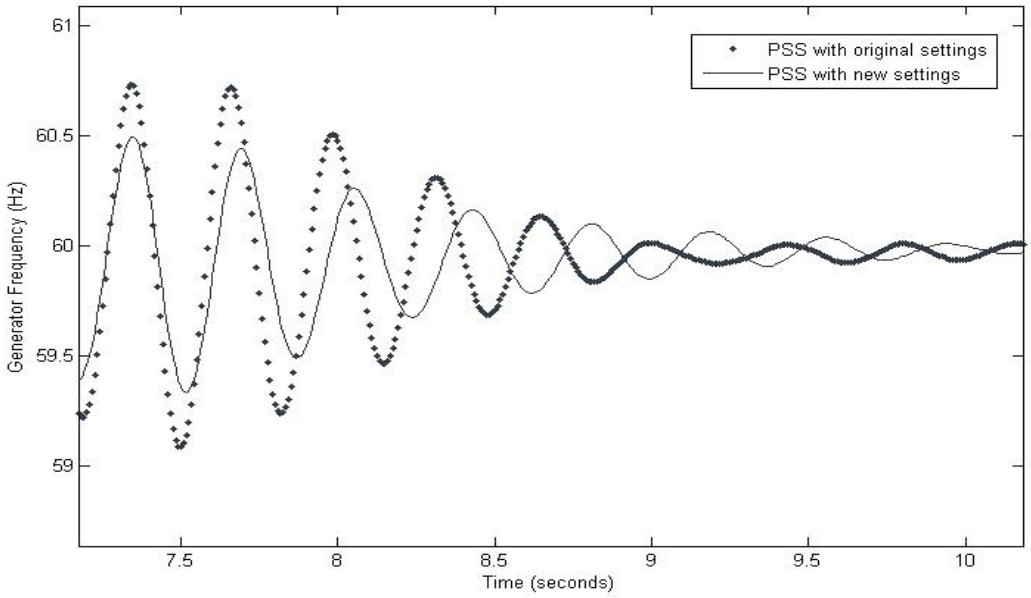

Fig 4.3 Comparison between the 95 generator speed with original and new PSS settings: Summer 2018 peak load case

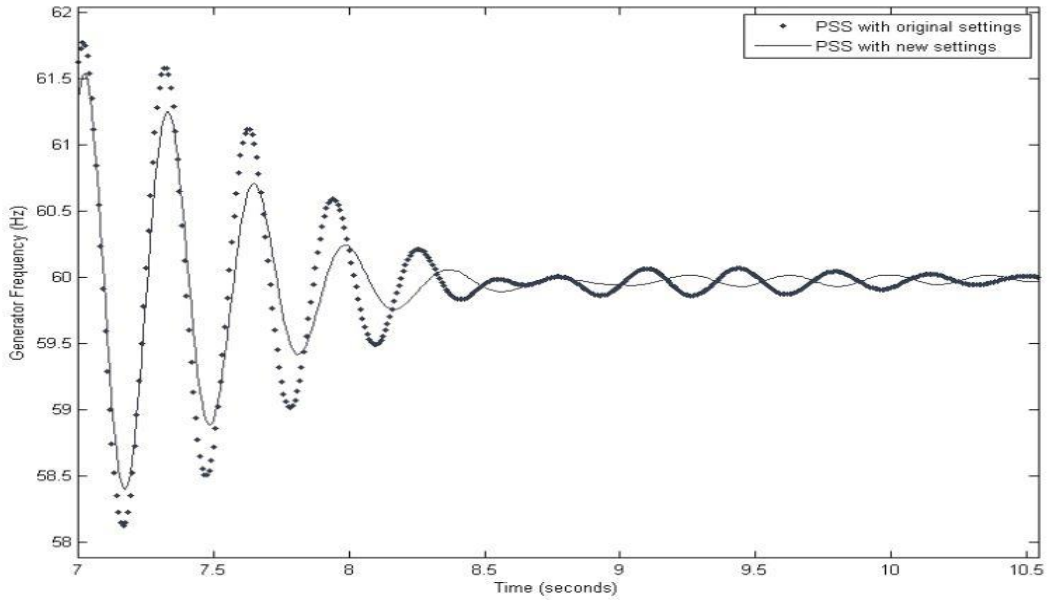

Fig 4.4 Comparison between the 96 generator speed with original and new PSS settings: Summer 2018 peak load case

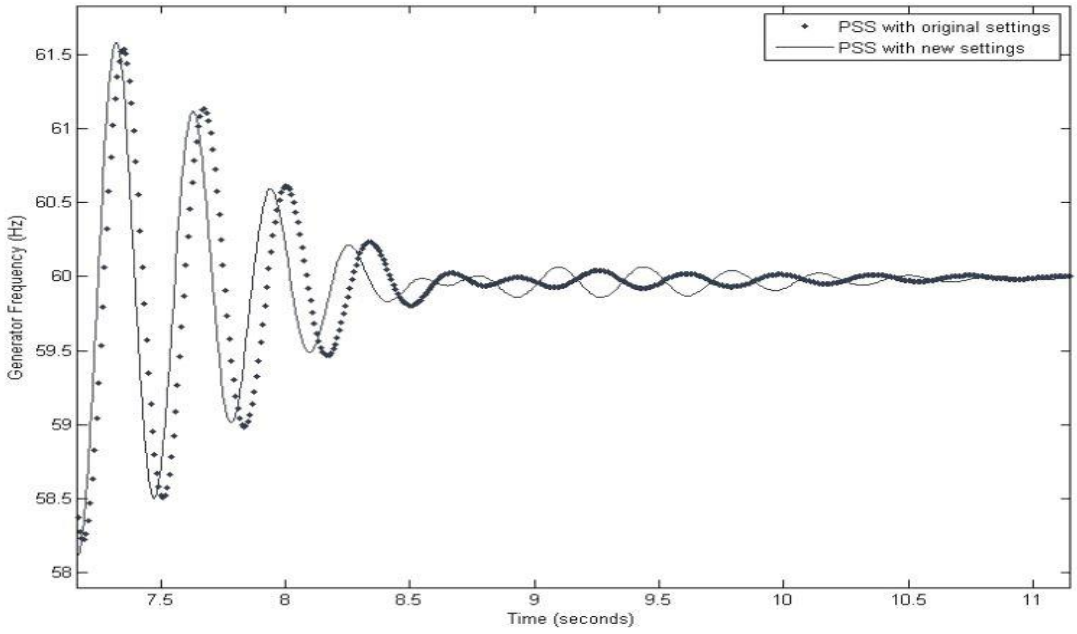

Fig 4.5 Comparison between the 97 generator speed with original and new PSS settings: Summer 2018 peak load case

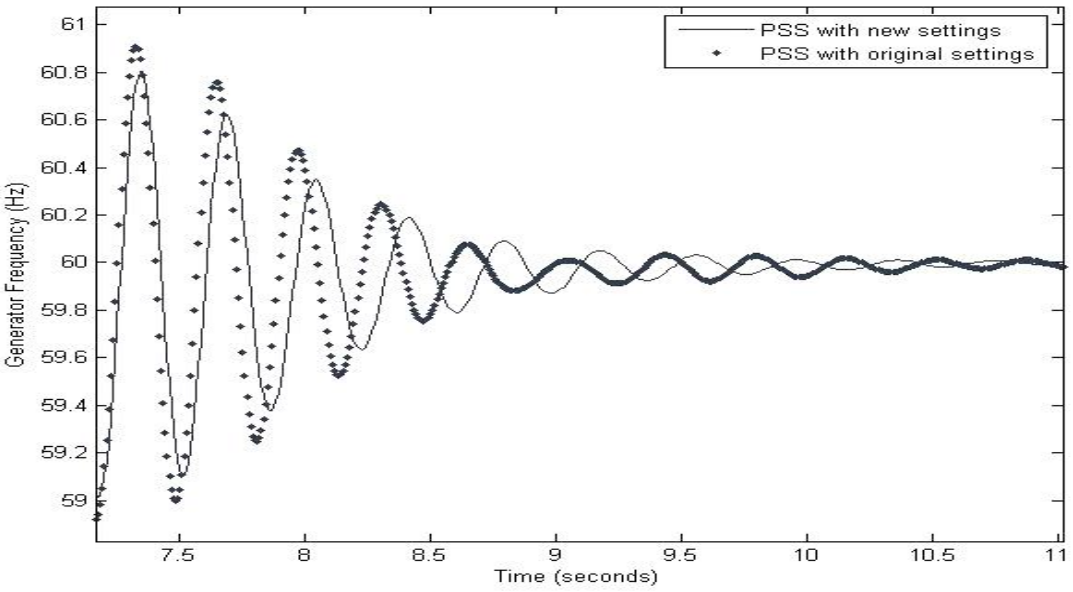

Fig 4.6 Comparison between the 98 generator speed with original and new PSS settings: Summer 2018 peak load case

The impact of PV penetration on selected buses (93 - 98) is observed. Eigenvalue analysis is carried out and reduction in damping performance is observed. Time domain simulations (test 5 – Appendix A) are also performed to see the oscillations which take longer time to damp. The PSS existing on the generators observed are retuned to damp the oscillations faster. The improvement in damping is observed graphically as the generator speed is plotted for the case where the PSS is at the original setting and the case where the PSS is retuned.

CHAPTER 5 CONCLUSIONS AND RECOMMENDATIONS FOR FUTURE WORK

5.1 Summative remarks

This thesis relates to photovoltaic generation in the electric power system under study. The impact of solar generation integration on power system dynamics is studied and evaluated. High photovoltaic solar penetration results in potentially problematic low system damping operating conditions. This is the case because the power system damping provided by conventional generation may be insufficient due to:

- Reduced system inertia
- Change in power flow patterns affecting synchronizing capability in the AC system

This occurs because conventional generators are rescheduled or shut down to allow for the increased solar production. The effects of high solar PV generation are observed using eigenvalue analysis and time domain simulations.

5.2 Conclusions

Spring 2010 light load case:

- The eigenvalue analysis (Table 3.4) shows poorly damped modes in the system with high levels of PV generation and the damping worsens as the PV generation increases. For the spring 2010 light load case, the dominant mode associated with bus 91 is the critically damped mode and the 50% PV generation case shows it's damping as low as 2.61% (Table 3.4).
- Prony analysis (time domain) identifies the poorly damped mode as mode 6 (Table 3.7).

- On retuning, the PSS existing on the generator at bus 91, the damping is improved and is seen graphically in Fig 3.4.

Summer 2018 peak load case:

- The eigenvalue analysis (Table 4.2) shows the poorly damped modes in the system with high levels of PV generation and the damping worsens as the PV generation increases. For the summer 2018 peak load case, the dominant mode associated with buses 93 to 98 show the critically damped modes (Table 4.2).
- Prony analysis (time domain) identifies the poorly damped modes (Tables 4.3 – 4.7) which correspond to the modes in Table 4.2.
- On retuning the PSSs existing on generator at bus 94, the damping is improved and is seen graphically in Fig 4.1. (Similar graphs are generated for other buses in the summer case and the improvement in damping is observed).

5.3 Recommendations for future work

Future work may involve the following:

- Steps to change the PSS settings as obtained after retuning the PSSs on the generators should be enumerated and identified.
- The spring light load data and summer peak load data (data of recent years for the spring case) should be updated.
- The impact of PV generation on buses outside of Arizona should be analyzed. And the effect of a change in PSS settings on system damping should be evaluated.

REFERENCES

[1] S. Eftekharnejad, V. Vittal, G. T. Heydt, B. Keel, J. Loehr, "Impact of Increased Penetration of Photovoltaic Generation on Power Systems," To appear in the *IEEE Transactions on Power Systems*, 2014.

[2] E. V. Larsen and D. A. Swann, "Applying Power System Stabilizers – Part I: General Concepts," *IEEE Transactions on Power Apparatus and Systems*, vol. PAS-100, No. 6, pp. 3017-3024, June 1981.

[3] E. V. Larsen and D. A. Swann, "Applying Power System Stabilizers – Part II: Performance Objectives and Tuning Concepts," *IEEE Transactions on Power Apparatus and Systems*, vol. PAS-100, No. 6, pp. 3025-3033, June 1981.

[4] E. V. Larsen and D. A. Swann, "Applying Power System Stabilizers – Part III: Practical Considerations," *IEEE Transactions on Power Apparatus and Systems*, vol. PAS-100, No. 6, pp. 3034-3046, June 1981.

[5] SSAT version 12.0 User's Manual, Powertech Labs, Inc., April 2012.

[6] TSAT version 12.0 User's Manual, Powertech Labs, Inc., April 2012.

[7] J. C. H. Peng, N. K. C. Nair, A. L. Maryani, A. Ahmad, "Adaptive Power System Stabilizer Tuning Technique for Damping Inter-Area Oscillations," *Proceedings of the IEEE Power and Energy Society General Meeting*, July 2010.

[8] O. Abedinia, M. S. Naderi, A. Jalili, B. Khamenehpour, "Optimal Tuning of Multi-machine Power System Stabilizer Parameters Using Genetic Algorithm," *International Conference on Power System Technology (POWERCON)*, October 2010.

[9] P. M. Anderson and A. A. Fouad, *Power System Control and Stability*, Institute of Electrical and Electronics Engineers, Inc., 2003.

[10] P. Kundur, *Power System Stability and Control*, McGraw-Hill, New York, 1994.

[11] PSLF version 18.1_01 User's Manual, General Electric International, Inc., October 2012.

[12] J. F. Hauer, C. J. Demeure, L. L. Scharf, "Initial Results in Prony Analysis of Power System Response Signals," *IEEE Transactions on Power Systems,* vol. 5, No. 1, February 1990.

[13] Liu Weiping, Lin Miaoshan, "Research and Application of High Concentrating Solar Photovoltaic System," *IEEE Second International Conference on Consumer Electronics*, Communications and Networks (CECNet), April 2012.

[14] C. T. Hsu, L. J. Tsai, T. J. Cheng, C. S. Chen, "Solar PV Generation System Controls for Improving Voltage in Distribution Network," *IEEE Second International Symposium* on Next-Generation Electronics (ISNE), February 2013.

[15] Shuhui Li, Huiying Zheng, "Energy Extraction Characteristic Study of Solar Photovoltaic Cells and Modules," *Power and Energy Society General Meeting*, IEEE Publications, July 2011.

[16] C. Hanley, G. Peek, J. Boyes, G. Klise, J. Stein, D. Ton, Tien Duong, "Technology Development Needs for integrated Grid-connected PV Systems and Electric Energy Storage," *Photovoltaic Specialists Conference*, IEEE Publications, Piscataway NJ, June 2009.

[17] P. M. Jansson, R. A. Michelfelder, V. E. Udo, G. Sheehan, S. Hetznecker, M. Freeman, "Integrating Large-Scale Photovoltaic Power Plants into the Grid," *Energy 2030 Conference*, IEEE Publications, November 2008.

[18] Anonymous, "Renewable Portfolio Standards," *Wikipedia.*

http://en.wikipedia.org/w/index.php?title=Renewable_portfolio_standard&oldid=607098287

[19] Liu Haifeng, Jin Licheng, D. Le, A. A. Chowdhury, "Impact of High Penetration of Solar Photovoltaic Generation on Power System Small Signal Stability," *International Conference on Power System Technology*, IEEE Publications, October 2010.

[20] Yi Zhang, Zhu Songzhe, R. Sparks, I. Green, "Impacts of Solar PV Generators on Power System Stability and Voltage Performance," *IEEE Power and Energy Society General Meeting*, July 2012.

[21] B. Tamimi, C. Canizares, K. Bhattacharya, "Modeling and Performance Analysis of Large Solar Photovoltaic Generation on Voltage Stability and Inter-area Oscillations," *IEEE Power and Energy Society General Meeting*, July 2011.

[22] DSA Tools TSAT Model Manual, *Powertech Labs Inc.*, March 2013.

[23] A. Pethe, V. Vittal, G. T. Heydt, "Evaluation and Mitigation of Oscillations Arising from High Solar Penetration due to Low Conventional Generation," *Proc. North American Power Symposium*, Pullman, WA, September 2014.

APPENDIX A

TASKS CARRIED OUT FOR SHUTTING DOWN GENERATORS

Test 1: Shutting down the CT and GT units to accommodate PV generation

A test was done to evaluate the reduction of combustion turbine (CT) and gas turbine (GT) generation. This task deals with altering the economic generation scheduling. Since the GT and CT units have relatively high operating costs, these types of conventional generator units are shut down to account for the additional PV generation. The PV is added in varying amounts (30%, 40%, and 50%) and equal amounts of generation are backed off from conventional generators. The generators that are selected to be shut down belong to the CT and GT type.

Test 2: Shutting down an aging coal unit

The generating units at an aging coal generation station are shut down in order to account for the additional PV generation. The units are shut down taking into consideration their location, participation factor and the type of plant.

Test 3: Shutting down alternative aging coal units

Alternative aging coal units in the area under study are shut down in order to account for the additional PV generation. The units are shut down taking into consideration their location, participation factor and the type of plant.

Test 4: Steps carried out for PSS tuning for the summer 2018 peak load case

- Using SSAT, the frequency response of the transfer function for the dominant mode at buses 93 to 98 without the PSS is plotted.

- At the frequencies of the respective mode, the corresponding phase lags are obtained.
- For the obtained phase lags, the lead / lag time constants T_1, T_2, T_3, T_4 are calculated using a MATLAB code for PSS design shown below:

$$f = frequency\ of\ mode$$

$$\omega = 2\pi f$$

$$\theta = \frac{-(phase\ lag)\pi}{180 \times 2}$$

$$\alpha = \frac{(1 + \sin\theta)}{(1 - \sin\theta)}$$

$$\tau = \frac{1}{\omega\sqrt{\alpha}}$$

with α and τ being the lead / lag time constants, and these expressions are in Hz, r/s, degrees and seconds.

Test 5: Time domain analysis

Time domain analysis is conducted using the TSAT. A three-phase fault is created on the bus which is electrically closest to bus whose behavior is observed since such a fault affects the critically damped modes the most. The fault is cleared after 6 cycles. The behavior of the generator at the selected bus is monitored.

APPENDIX B

MATLAB CODE FOR PSS TUNING – LARSEN AND SWANN METHOD

```
%%%%%%%%%%%%%%%%%%%%%%%%%%%%%%%%%%%%%%%%%%%%%%%
%%%%%%%%%%%
%% Purpose:  Draw the phase characteristic of PSS vs. phase lag between
%%           exciter input and electrical toque.
%% Author:   Shu Liu
%% Date:     10/20/2003
%% Input:    Asys.ssa - Linear analysis result from MASS.
%% Output:   Figure.
%% Variable:
%%           nModeN          - The number of the total states.
%%           nStateN         - The number of the states for every unit.
%%           nUnitN          - The number of the units.
%%           A, B, C, D      - System matrix A, B, C, D.
%%           T1, T2, T3, T4, T5 - Time constants of PSS control block.
%% Note:     This code is used for the PSS at Unit 1. For PSSs at other units, certain
changes need to be made according to the comments in the following code.
%%%%%%%%%%%%%%%%%%%%%%%%%%%%%%%%%%%%%%%%%%%%%%%
%%%%%%%%%%%
clc;
clear all;
close all;
%%%% Begin to set the value of variable
nModeN = 36;                %% The number of the states
nStateN = 9;                %% The number of the states for every unit.
nUnitN = 4;                 %% The number of the units.
A = zeros(nModeN,nModeN);
B = zeros(nModeN,1);
C = zeros(1,nModeN);
D = zeros(1,1);
%% PSS tuning for nth unit: select accordingly
PSS_ID = 1
%% PSS lead-lag parameter tuning
T1 =0.1;% 0.6179;
T2 =0.1;% 0.01;
T3 =0.1;% 0.6172;
T4 =0.1;% 0.05182;
T5 = 10;
%%%% End of setting the value of variable
```

```
%%%% Begin to Read data from files.

%% Read A matrix from file
fName = strcat('Project3.sma');
fID = fopen(fName,'r');
%% skip first 21 lines
for n=1:21
   strTemp=fgets(fID);
end
% read Asys from file
for n=1:nModeN
   for m=1:nModeN
      fTemp1=fscanf(fID,'%g',1);
      A(m,n)=fTemp1;
   end
end
fclose(fID);
%%%% End of Read data from files.

%%%% Begin to set B, C, D matrix

%% B matrix
for n = 1:nUnitN %4
   for m = 1:nStateN % 9
      B((n-1)*nStateN+m,1) = 0;
   end
   if (n==PSS_ID)            %% For PSS at Unit 1, (n==1)
      B((n-1)*nStateN+8,1) = 0.1;
      B((n-1)*nStateN+9,1) = 1.0;
   end
end

%% C matrix
C = (-2*6.5*9)*A((PSS_ID-1)*nStateN+1,:);         %% For PSS at Unit - under
consideration, A(PSS_ID,:)
for k = 1:nUnitN
   C(1,(k-1)*nStateN+1) =  0;              %% Set all the element about speed to 0.
end
%% D matrix
D(1,1) = 0;
%%%% End of setting B, C, D matrix
```

```
%%%% Begin to calculate the transform function of the system with no PSS.
%% Set Ap, Bp, Cp, Dp
%% remove state equations corresponding to speed and angle
Ap = A;
Ap([1 2 10 11 19 20 28 29],:)=[];
Ap(:,[1 2 10 11 19 20 28 29])=[];
Bp = B;
Bp([1 2 10 11 19 20 28 29],:)=[];
Cp = C;
Cp(:,[1 2 10 11 19 20 28 29])=[];
Dp = D;

GEP = ss(Ap,Bp,Cp,Dp);
%%%% End of calculating the transform function of the system with no PSS.

%%%% Begin to draw the phase characteristic of the GEP.
[SysMAG,SysPHASE,SysW] = bode(GEP);
% bode(GEP);
SysW = SysW';
SysW = (1/(2*pi))*SysW;
for n = 1:length(SysW)
   fTemp = SysPHASE(n);
   fSysPhase(n) = -fTemp;
end
figure('Color',[1 1 1])
axes1 = axes('Parent',figure(1),'FontSize',12);
plot(SysW,fSysPhase,'LineWidth',1.5);
axis([0 2 0 140]);
grid on;
hold on;
%%%% End of drawing the phase characteristic of the GEP.
%%
yy = fSysPhase(1:30);
xx = 2*pi*SysW(1:30);
 xx(1:25) = xx(1:25).*1.8;
%  xx(29:32) = xx(29:32).*2.2;
%%%% End of finding the value of the time constants and gain of PSS

%%(180/pi)*(pi/2 - atan2(10*x,1) + atan2(T1*x,1) - atan2(T2*x,1) + atan2(T3*x,1) -
atan2(T4*x,1) )
```

```
%% Fit: 'untitled fit 1'.
[xData, yData] = prepareCurveData( xx, yy );

% Set up fittype and options.
ft = fittype( '(180/pi)*(pi/2 - atan2(10*x,1) + atan2(T1*x,1) - atan2(T2*x,1) +
atan2(T3*x,1) - atan2(T4*x,1) )', 'independent', 'x', 'dependent', 'y' );
opts = fitoptions( ft );
opts.Display = 'Off';
opts.Lower = [0.01 0.01 0.01 0.01];
opts.Robust = 'LAR';
opts.StartPoint = [0.254282178971531 0.814284826068816 0.243524968724989
0.929263623187228];
opts.Upper = [Inf Inf Inf Inf];

% Fit model to data.
[fitresult, gof] = fit( xData, yData, ft, opts );
Tval = coeffvalues(fitresult);
T1 =Tval(1);
T2 =Tval(2);
T3 =Tval(3);
T4 =Tval(4);
% Plot fit with data.
figure( 'Name', 'untitled fit 1' );
h = plot( fitresult, xData, yData );
legend( h, 'yy vs. xx', 'untitled fit 1', 'Location', 'NorthEast' );
% Label axes
xlabel( 'xx' );
ylabel( 'yy' );
grid on
%%
%%%% Begin to calculate the transform function of the PSS.
[PssMAG,PssPHASE,PssW] =
bode([T1*T3*T5,(T3*T5+T1*T5),T5,0],[T2*T4*T5,(T2*T5+T4*T5+T2*T4),(T2+T4+T
5),1]);
%
bode([T1*T3*T5,(T3*T5+T1*T5),T5,0],[T2*T4*T5,(T2*T5+T4*T5+T2*T4),(T2+T4+T
5),1]);
PssW = PssW';
PssW = (1/(2*pi))*PssW;
for n = 1:length(PssW)
   fTemp = PssPHASE(n);
```

```
    fPssPhase(n) = fTemp;
end
figure(1)
plot(PssW,fPssPhase,'r','LineWidth',1.5);
hold all;
axis([0 2 0 140]);
if PSS_ID ==1
    Ta2 = 0.138 ;
    Ta1 = 1.2683 ;
elseif PSS_ID ==2
    Ta2 = 0.1446 ;
Ta1 = 1.2102 ;
elseif PSS_ID ==3
    Ta2 = 0.1396 ;
    Ta1 = 1.254 ;
elseif PSS_ID ==4
    Ta2 = 0.1459;
    Ta1 = 1.1999 ;
end
Ta3 = Ta1; Ta4 = Ta2; Ta5 = T5;
k1k6pss  =
tf([Ta1*Ta3*Ta5,(Ta3*Ta5+Ta1*Ta5),Ta5,0],[Ta2*Ta4*Ta5,(Ta2*Ta5+Ta4*Ta5+Ta2*T
a4),(Ta2+Ta4+Ta5),1]);
[PssMAG2,PssPHASE2,PssW] = bode(k1k6pss);
PssW = PssW';
PssW = (1/(2*pi))*PssW;
for n = 1:length(PssW)
    fTemp = PssPHASE2(n);
    fPssPhase2(n) = fTemp;
end
% Create axes
plot(PssW, fPssPhase2,'k','LineWidth',1.5);
axis([0 2 0 140]);
xlabel('Frequency (Hz)','FontSize',14);

% Create ylabel
ylabel('Phase angle (degrees)','FontSize',14);

% Create title
ttl = ['PSS Tuning at Generator' ,' ', num2str(PSS_ID)];
title(ttl,'FontSize',16);
```

```
legend1 = legend('PHASE LAG TO BE COMPENSATED', 'PSS PHASE LEAD - Larsen
& Swann', 'PSS PHASE LEAD - K1-K6 method')
% Create legend
set(legend1,...
   'Position',[0.696629832957958 0.148427164672403 0.203891000375375
0.0916953851010209],...
   'FontSize',14);

%%%% End of calculating the transfer function of the PSS.

%%%% Begin to find the value of the time constants and gain of PSS
Tval

% figure(5)
%
rlocus(GEP*tf([T1*T3*T5,(T3*T5+T1*T5),T5,0],[T2*T4*T5,(T2*T5+T4*T5+T2*T4),(
T2+T4+T5),1]))
% figure(6)
%
bode(GEP*tf([T1*T3*T5,(T3*T5+T1*T5),T5,0],[T2*T4*T5,(T2*T5+T4*T5+T2*T4),(T
2+T4+T5),1]))
%% compare final results
P1 = xlsread('LS_method_PSS.xls');
P2 = xlsread('K1_K6_method_PSS.xls');
P3 = xlsread('NoPSS.xls');
figure(4)

subplot(3,1,1) ;
plot(P1((8:end),1), P1((8:end),2),'k','LineWidth',1.5);
hold all;
grid on;
subplot(3,1,2) ;
plot(P1((8:end),1), P1((8:end),3),'k','LineWidth',1.5);
hold all;
grid on;
subplot(3,1,3) ;
plot(P1((8:end),1), P1((8:end),4),'k','LineWidth',1.5);
hold all;
grid on;
% subplot(4,1,4) ;
```

```
% plot(P1((8:end),1), P1((8:end),5),'k','LineWidth',1.5);
% hold all;
% grid on;
figure(4)
subplot(3,1,1) ;
plot(P2((8:end),1), P2((8:end),2),'r','LineWidth',1.5);
subplot(3,1,2) ;
plot(P2((8:end),1), P2((8:end),3),'r','LineWidth',1.5);
subplot(3,1,3) ;
plot(P2((8:end),1), P2((8:end),4),'r','LineWidth',1.5);
% subplot(4,1,4) ;
% plot(P2((8:end),1), P2((8:end),5),'r','LineWidth',1.5);
figure(4)
subplot(3,1,1) ;
plot(P3((8:end),1), P3((8:end),2),'b','LineWidth',1.5);
title('Generator at bus#1');
xlabel('Time (s)');
ylabel('Rotor angle {\delta} (deg)');
legend('Larsen & Swann Method PSS Design', 'K1-K6 Method PSS Design','No PSS')
hold all;
subplot(3,1,2) ;
plot(P3((8:end),1), P3((8:end),3),'b','LineWidth',1.5);
title('Generator at bus#2');
xlabel('Time (s)');
ylabel('Rotor angle {\delta} (deg)');
legend('Larsen & Swann Method PSS Design', 'K1-K6 Method PSS Design','No PSS')
subplot(3,1,3) ;
plot(P3((8:end),1), P3((8:end),4),'b','LineWidth',1.5);
% subplot(4,1,4) ;
% plot(P3((8:end),1), P3((8:end),5),'b','LineWidth',1.5);
title('Generator at bus#4');
xlabel('Time (s)');
ylabel('Rotor angle {\delta} (deg)');
legend('Larsen & Swann Method PSS Design', 'K1-K6 Method PSS Design','No PSS')

%% compARE PLOTS at SS Limit
Pa1 = xlsread('compare at ss limit LS method.xls');
Pa2 = xlsread('compare at ss limit K1K6 method.xls');
% P3 = xlsread('NoPSS.xls');
figure(7)
subplot(3,1,1) ;
```

```
plot(Pa1((8:end),1), Pa1((8:end),2),'k','LineWidth',1.5);
hold all;
grid on;
subplot(3,1,2) ;
plot(Pa1((8:end),1), Pa1((8:end),3),'k','LineWidth',1.5);
hold all;
grid on;
subplot(3,1,3) ;
plot(Pa1((8:end),1), Pa1((8:end),4),'k','LineWidth',1.5);
hold all;
grid on;
% subplot(4,1,4) ;
% plot(P1((8:end),1), P1((8:end),5),'k','LineWidth',1.5);
% hold all;
% grid on;
figure(7)
subplot(3,1,1) ;
plot(Pa2((8:end),1), Pa2((8:end),2),'r','LineWidth',1.5);
title('Generator at bus#1');
xlabel('Time (s)');
ylabel('Rotor angle {\delta} (deg)');
legend('Larsen & Swann Method PSS Design', 'K1-K6 Method PSS Design','No PSS')
subplot(3,1,2) ;
plot(Pa2((8:end),1), Pa2((8:end),3),'r','LineWidth',1.5);
title('Generator at bus#2');
xlabel('Time (s)');
ylabel('Rotor angle {\delta} (deg)');
legend('Larsen & Swann Method PSS Design', 'K1-K6 Method PSS Design','No PSS')
subplot(3,1,3) ;
plot(Pa2((8:end),1), Pa2((8:end),4),'r','LineWidth',1.5);
title('Generator at bus#4');
xlabel('Time (s)');
ylabel('Rotor angle {\delta} (deg)');
legend('Larsen & Swann Method PSS Design', 'K1-K6 Method PSS Design')
```